Single-walled carbon nanotube networks for flexible and printed electronics

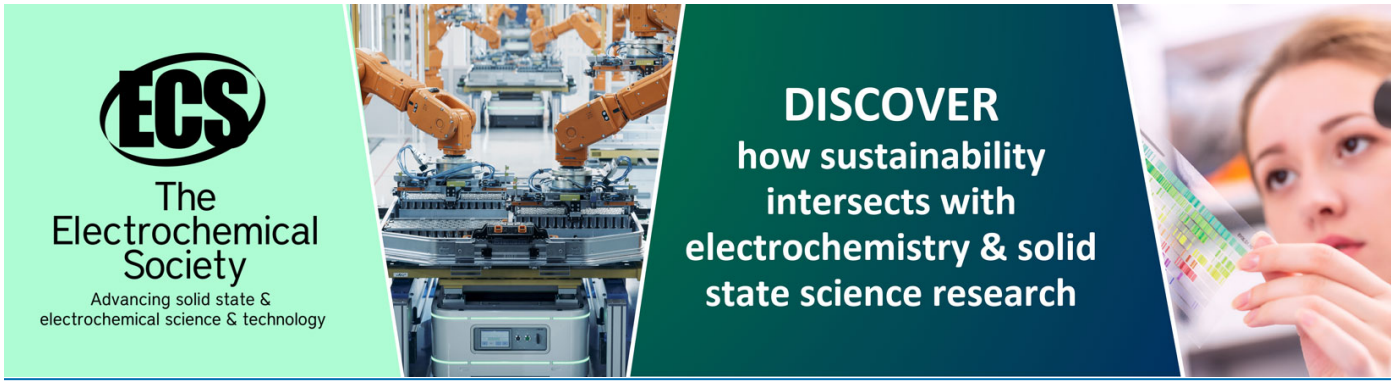

OPEN ACCESS
IOP Publishing
Semiconductor Science and Technology
Semicond. Sci. Technol. **30** (2015) 074001 (20pp)
doi:10.1088/0268-1242/30/7/074001

Single-walled carbon nanotube networks for flexible and printed electronics

Jana Zaumseil

Universität Heidelberg, Institute for Physical Chemistry, 69120 Heidelberg, Germany

E-mail: zaumseil@uni-heidelberg.de

Received 27 February 2015, revised 17 April 2015
Accepted for publication 6 May 2015
Published 9 June 2015

Abstract

Networks of single-walled carbon nanotubes (SWNTs) can be processed from solution and have excellent mechanical properties. They are highly flexible and stretchable. Depending on the type of nanotubes (semiconducting or metallic) they can be used as replacements for metal or transparent conductive oxide electrodes or as semiconducting layers for field-effect transistors (FETs) with high carrier mobilities. They are thus competitive alternatives to other solution-processable materials for flexible and printed electronics. This review introduces the basic properties of SWNTs, current methods for dispersion and separation of metallic and semiconducting SWNTs and techniques to deposit and pattern dense networks from dispersion. Recent examples of applications of carbon nanotubes as conductors and semiconductors in (opto-)electronic devices and integrated circuits will be discussed.

Keywords: carbon nanotubes, transistors, printed

(Some figures may appear in colour only in the online journal)

1. Introduction

Among the various choices of materials for printed and flexible electronics, single-walled carbon nanotubes (SWNTs) are unique in the sense that they can be either metallic or semiconducting. Metallic SWNTs can withstand larger current densities than copper or aluminium [1] and their electrical conductivity is extremely high [2]. Semiconducting SWNTs are intrinsically ambipolar and show equal hole and electron mobilities depending on environmental conditions [3, 4]. Carrier mobilities in individual carbon nanotubes reach tens of thousands of $cm^2\,V^{-1}\,s^{-1}$ at room temperature [5, 6]. They are both highly flexible and strong [7]. Networks or thin films of SWNTs are extremely stretchable without noticeable changes in conductivity [8]. They are environmentally stable and durable, and can be processed from dispersions at low temperatures, which makes them suitable for printing on plastic substrates. Although the conductivities and carrier mobilities in SWNT networks, which are limited by nanotube–nanotube junctions are much lower than those in individual nanotubes, sheet resistances of less than 100 Ω/sq [9, 10] and effective mobilities of more than $100\,cm^2\,V^{-1}\,s^{-1}$ [11, 12] are achievable while maintaining high transparency. Thus, SWNTs seem to be the perfect choice for printable, flexible and stretchable electronics. Unfortunately, many of these favourable properties are not easily or simultaneously accessible. The fundamental problem that prevented SWNTs from reaching widespread use in electronics over the past decade was the fact that all methods for SWNT growth produce a statistical mixture of about 1/3 metallic and 2/3 semiconducting nanotubes with a variety of diameters and therefore electronic properties [13]. In order to be able to use SWNTs for either highly conductive electrodes or as semiconducting layers, it is necessary to separate the different types and create stable and reproducible inks/dispersions for further device processing. There has been tremendous progress in this field over the last few years [14–17]. At least for semiconducting SNWTs the purification problem seems to be solved and it is now possible to tap the full potential of solution-processed thin film carbon nanotube electronics. In this review we will describe current methods for dispersing and sorting semiconducting nanotubes as well as SWNT deposition and patterning techniques. We discuss the

application of SWNT networks as conductors for electrodes and as semiconductors in field-effect transistors (FETs) for large area and printed electronics. Examples of integrated circuits based on SWNTs and novel SWNT light-emitting devices will illustrate the recent progress.

2. Brief carbon nanotube basics

SWNTs are conceptually viewed as rolled-up sheets of graphene, and their electronic properties can be derived from those of graphene with additional boundary conditions. Each nanotube can be described by its chiral vector $\boldsymbol{C_h} = n \cdot \boldsymbol{a_1} + m \cdot \boldsymbol{a_2}$ with $\boldsymbol{a_1} = (a\sqrt{3}/2,\ a/2)$ and $\boldsymbol{a_2} = (a\sqrt{3}/2,\ -a/2)$ as the unit vectors (see figure 1(a)) with the hexagonal lattice constant $a = 0.246$ nm of the graphene sheet. The chiral vector determines how the graphene sheet is rolled-up. Hence, the pair of indices (n, m) is used to identify each SWNT species. The chiral angle and diameter of the nanotubes can be calculated directly from these values [18]. Nanotubes with $n = m$, e.g. (6, 6), are called armchair nanotubes and those with $m = 0$, e.g. (10, 0), are zigzag nanotubes. Both types are achiral, that is they have a mirror plane, while all other SWNTs are chiral (see figure 1(b)). An (8, 4) SWNT is the mirror image of a (4, 8) nanotube. This led to the somewhat confusing usage of the word 'chiralities' for all different species of nanotubes, that is, for nanotubes with different pairs of n and m.

Due to the introduction of periodic boundary conditions for the wave functions of the infinite graphene sheet in the circumferential direction, the allowed wave vectors around the nanotube circumference are quantized, that is they can take only a set of discrete values. The electronic properties of SWNTs depend directly on their chiral vector. The simplest description follows the zone-folding approximation, which introduces so-called cutting lines for the allowed wave vector values that run across the reciprocal lattice of the graphene [19, 20]. When at least one cutting line goes through the K or K' point of the graphene the resulting nanotube is metallic. This is the case for all armchair nanotubes and for those with $(m\text{-}n)\text{mod}(3) = 0$. All other nanotubes with $(m\text{-}n)\text{mod}(3) = 1$ or 2 are semiconducting.

The selection of the possible states in k-space leads to the characteristic density of states (DOS) distribution of carbon nanotubes. It is dominated by sharp peaks, i.e. the van Hove singularities (see figure 1(c)), which are a key feature of the DOS of 1D conductors. This narrow distribution of occupied and unoccupied states is the origin of the characteristically narrow absorption and photoluminescence peaks of SWNTs [21] (see figure 2(a)). The energy differences between corresponding van Hove singularities (i.e. E_{11}, E_{22} etc) scale with the inverse of the diameter. They are plotted in the Kataura plot [22, 23] versus diameter and sorted by type. This enables the identification of metallic and semiconducting nanotubes from absorption spectra or radial breathing modes in resonant Raman spectra if the diameter range of the nanotubes is known [24]. The E_{11} transitions, or bandgaps, of semiconducting nanotubes (diameter 0.7–2 nm) range from

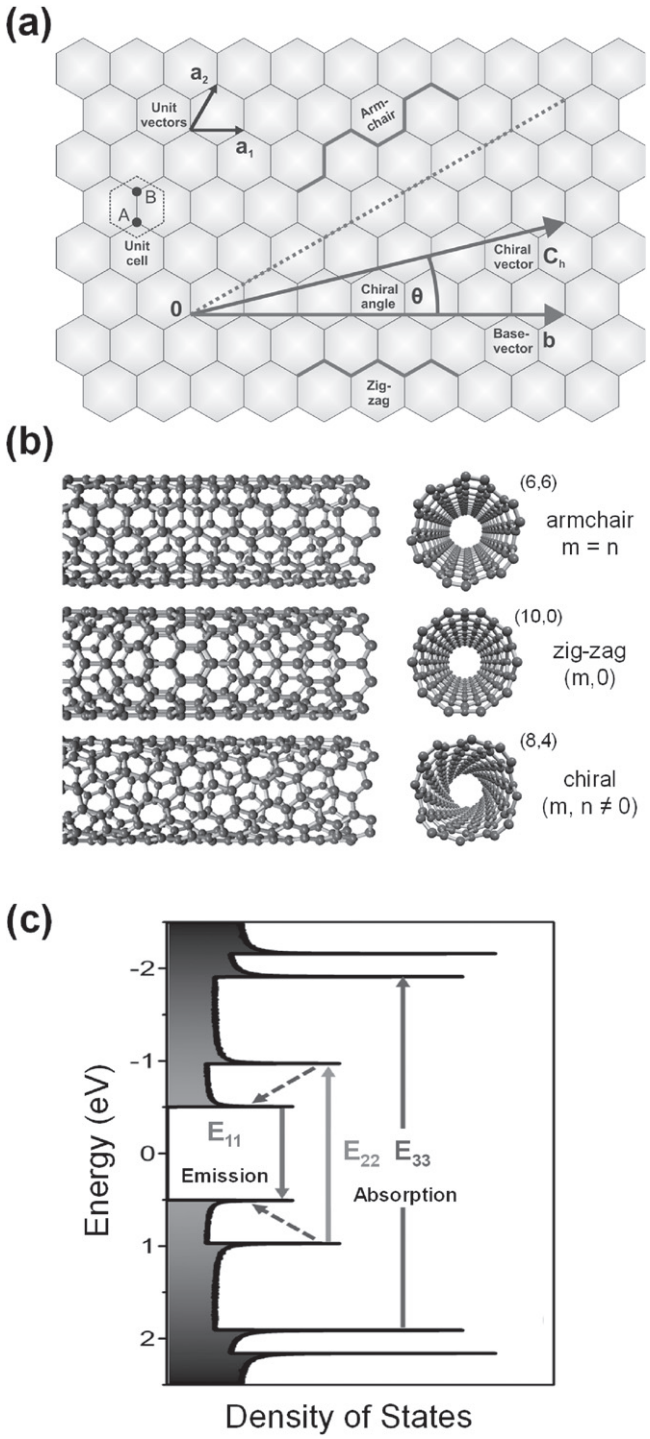

Figure 1. (a) Illustration of chiral vector $\boldsymbol{C_h}$ and chiral angle θ of a (6, 2) SWNT within a graphene sheet. The armchair ($\theta = 30°$, $m = n$) and zigzag configuration ($\theta = 0°$, $n = 0$) are indicated. (b) Molecular structures of an armchair (6, 6), zigzag (10, 0) and chiral (8, 4) carbon nanotube. (c) Density of states (DOS) for a semiconducting SWNT, typical transitions for light absorption and emission are labelled (E_{11}, E_{22}, E_{33}).

about 1.1 eV to 0.4 eV (near-infrared), while the E_{22} transitions are between 2.2 eV and 0.7 eV (visible to near-infrared). Semiconducting carbon nanotubes show excitonic photoluminescence in the near-infrared (E_{11} transition), which can

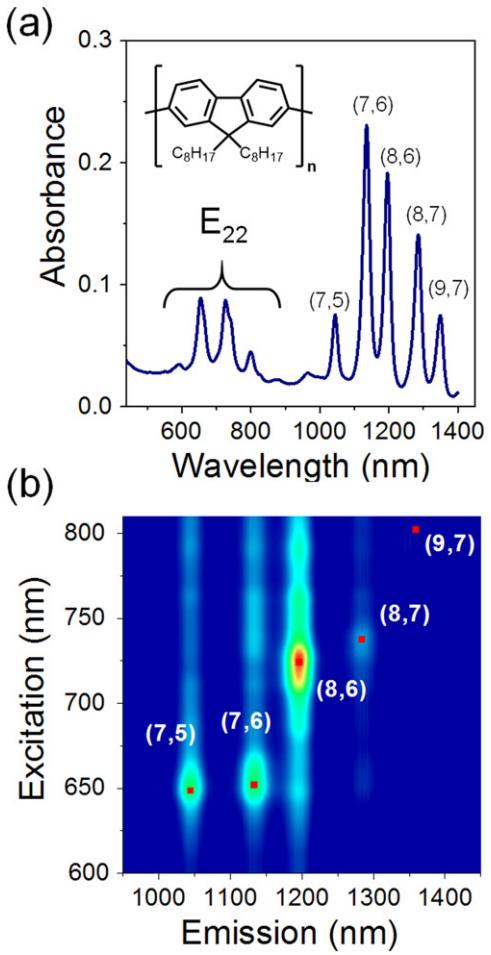

Figure 2. (a) Absorbance spectrum of a dispersion of semiconducting SWNTs selected from HipCO® nanotubes by dispersion with poly(9, 9-dioctylfluorene) (see inset) in toluene. The E_{11} transitions of five SWNT species (labelled) and the corresponding E_{22} transitions are evident. There are no absorption peaks for metallic nanotubes. (b) Excitation–emission map of the SWNT dispersion with each intensity peak corresponding to one of the five nanotube species.

be used to identify their species in photoluminescence excitation/emission maps [21]. An absorption spectrum and excitation–emission map of a sample of dispersed nanotubes that contains only five different types of semiconducting SWNTs is shown in figure 2.

3. Dispersion and sorting of carbon nanotubes

There are three major synthesis methods for producing SWNTs. The most common method is chemical vapour deposition with metallic catalyst particles such as iron or cobalt/molybdenum in the gas phase or on support materials (e.g. MgO). The carbon sources are, for example, CH_4, C_2H_4, ethanol or CO. Typical commercial processes like HipCO® [25] and CoMoCat® [26] produce SWNTs with relatively small diameters (0.7–1.2 nm). The CoMoCat® process is notable because it allows for preferential growth of the semiconducting (6, 5) and (7, 6) nanotubes, although some metallic nanotubes are still present. Another type of SWNT synthesis relies on the vapourization of carbon in an inert atmosphere by arc-discharge [27], laser ablation [28] or arc plasma jet [29]. These methods produce SWNTs with larger diameters usually in the range of 1–3 nm. Finally, the plasma torch method provides a comparable synthesis environment to the arc-discharge growth with high processing temperatures in the range of 1000–1200 °C [30, 31]. The high temperatures are created by a dc-driven or radio frequency-induced thermal plasma. Carbon containing precursor gases such as C_2H_4 are used in continuous flow together with metal catalysts like Fe, Co or Ni, or organometallic compounds like ferrocene or Fe$(CO)_5$. The plasma torch SWNT growth was developed into a highly economical process with large scale systems reaching outputs of several kilograms per day and high quality SWNTs with diameters of 1.2–1.6 nm.

These commercially available SWNTs come as raw powders containing SWNTs of various diameters and electronic type, some soot/amorphous carbon, and possibly metallic catalyst residue. For further processing the nanotubes must be dissolved or dispersed. Unfortunately, they are essentially insoluble in almost all organic solvents [32, 33]. The length of the nanotubes reduces the entropic gain from interacting with solvent molecules and the strong van der Waals forces between the SWNTs favour the formation of tight bundles. Nanotubes can be de-bundled through the application of strong shear forces, e.g. by sonication or mechanical milling, but they must be stabilized afterwards to prevent re-aggregation. This can be achieved in a number of ways that are well-known from other colloids. SWNTs can be stabilized in aqueous dispersions by surfactants or tensides. The surfactant molecules (e.g. sodiumdodecylsulphate (SDS) [34] or cholates [35]) form a micelle structure around the SWNTs with the hydrophobic tails pointing toward the nanotube and the ionic/hydrophilic headgroups toward the water. Another very efficient dispersing agent for SWNTs in water is single- or double-stranded DNA of any type [36, 37]. The interaction of the aromatic nucleotide bases with the nanotubes is strong and results in helical wrapping while the sugar-phosphate backbone creates a partially negative surface charge and thus electrostatic stabilization. After sonication or milling in the presence of the dispersing agent, the SWNT dispersions are centrifuged at high accelerations (usually above 200 00 g) to separate individualized SWNTs from bundles and other residues. Stable dispersions with high concentrations (few mg/ml) of individualized SWNTs can be obtained with surfactants or DNA, which is essential for creating printable SWNT inks. However, all of these dispersion processes are largely non-selective, and metallic and semiconducting SWNTs are dispersed in equal quantities.

The first attempts to separate SWNTs according to their metallicity or diameter were quite expensive and limited to very small amounts in the nanogram range, which severely limited their applicability [37–39]. The first efficient and scalable separation method was density gradient ultracentrifugation (DGU) of SWNTs that were dispersed in a mix of SDS and cholates. The separation relied on the different buoyant densities of the SWNTs including their surfactant

shell, which depend on the SWNT diameter but also its metallicity [40, 41]. A more recent approach is the use of classic gel-chromatography [42–45]. An agarose gel column is saturated with SWNTs dispersed in SDS, and a pure SDS solution is used as the eluent. The metallic nanotubes exhibit the weakest interaction with the agarose gel and are washed out first. Semiconducting nanotubes interact more strongly, depending on their diameter [46]. These differences can be enhanced by tuning the pH and temperature [47]. It is thus possible to create nearly single-species dispersions in a scalable and reproducible way. This accomplishment can be regarded as a true breakthrough in this field of research and enables a range of studies and applications that were impossible until then.

While gel-chromatography separates already dispersed SWNTs, it is also possible to start directly with the selective dispersion of only certain types of nanotubes. This is achieved by mixing the raw carbon nanotube powder with conjugated polymers in organic solvents such as toluene or xylene, as originally discovered by Nish *et al* [48]. Suitable conjugated polymers are polyfluorenes and polyfluorene copolymers [48–55], regio-regular polythiophenes [56, 57], and also polycarbazoles [58, 59]. All of these polymers preferentially disperse semiconducting SWNTs, although the degree of selectivity varies. During dispersion the SWNTs are wrapped by the polymer chains in order to maximize the π–π electron interaction of the polymer backbone and the nanotubes. The length of the alkyl-side-chains that make the polymers soluble in organic solvents determines to some degree the diameter of the preferentially stabilized carbon nanotubes. Longer side-chains lead to the dispersion of nanotubes with larger diameters [50, 56]. The yield and selectivity also depend on the solvent [60, 61] and the molecular weight of the polymer. Lower molecular weights increase the selectivity but decrease the yield of dispersion [62, 63]; a minimum chain length is required for effective dispersion [64]. The obtained concentrations of semiconducting SWNTs in polymer solution can vary from tens of ng/ml to hundreds of μg/ml. In all cases there is still a substantial amount of polymer in the dispersion, which helps to stabilize it. However, its presence would hinder charge transport in a film produced from such a dispersion, as the conjugated polymers exhibit orders of magnitude lower mobilities than the SWNTs. The majority of the unbound polymer can be removed by filtration of the dispersion and washing of the obtained SWNT film with a solvent. Alternatively, sedimentation of the nanotubes at ultrahigh centrifugation speeds (>250 000 g) creates a pellet that is recovered and rinsed with a clean solvent. The purified SWNTs can be redispersed in the pure solvent, e.g. toluene, and used for spincoating, drop-casting or printing. An elegant but synthetically more challenging route is the use of conjugated polymers that are degradable after the selection and dispersion step and can thus be removed easily and without residue [65–67]. A thorough overview of selective polymer dispersion has recently been given by Samanta *et al* [68].

4. Deposition of nanotube networks

A variety of techniques to deposit SWNTs from dispersion with different densities and degrees of alignment have been applied over the years. The most common lab technique for thin film deposition from solution, spincoating, requires quite high SWNT concentrations in order to obtain a reasonably dense surface coverage as shown in figure 3(a). Very often an adhesion promoter is used to increase coverage, such as 3-aminopropyltriethoxy silane (APTES) [69–71] or poly-L-lysine [72, 73]. Due to the centripetal forces during spincoating and the drying effects at the edges of the sample, the nanotube distribution is not completely uniform. Interestingly, longer nanotubes appear to become more abundant at larger distances from the center of the sample [74]. Other methods for large area deposition of SWNTs from dispersion include immersing a substrate with an adhesion layer in a SWNT dispersion, followed by rinsing [75–78], dip-coating [79, 80], spray-coating [81, 82], and Mayer rod or blade-coating [83, 84]. The latter can lead to a partial alignment of the SWNTs, which reduces the sheet resistance.

In general, good nanotube alignment is desirable especially for semiconducting SWNT networks. An easy way to obtain well-aligned SWNTs between two electrodes is the application of an electric field during drop-casting of the nanotube dispersion. Both high frequency alternating fields [85–88] and large dc fields [89, 90] are suitable (see figure 3(b)). Low concentrations of SWNTs are sufficient as deposition only takes place between the electrodes, which also avoids post-deposition patterning. However, the uniformity of deposition depends critically on the dispersion quality and this technique is not scalable. Evaporation assembly techniques that rely on the lyotropic liquid crystalline properties of SWNT dispersions at high concentrations are slightly more suitable for alignment of nanotubes over large areas. Under controlled drying conditions, aligned thin stripes or films of nanotubes can be deposited from SWNT dispersion on semi-immersed substrates [91–94]. The nanotubes assemble parallel to the drying line and good linear SWNT densities (10–20 μm^{-1}) with high degrees of alignment are achieved. Strong alignment and very high SWNT densities of up to 500 μm^{-1} can be obtained by applying the Langmuir–Schaefer method to compress nanotubes on a water surface before transfer [95].

For application in field-effect transistors and circuits most of the techniques described above require the post-deposition patterning of the SWNT films to reduce leakage currents and device cross-talk. This can be done by selective removal of SWNTs with oxygen plasma while other areas are protected, e.g. by photoresist. Nevertheless, as the purified source material is expensive, more frugal, additive deposition techniques, i.e. direct printing of SWNTs, are desirable. Printing methods that require high viscosity inks such as flexography (viscosity range 0.05–0.5 Pa s), gravure (0.01–0.2 Pa s), offset (5–100 Pa s) and screen printing (0.5–50 Pa s) [96] have so far been rarely reported in literature, although commercial sources for high viscosity (unsorted) SWNT inks exist. For type-sorted nanotube dispersions the necessary high SWNT

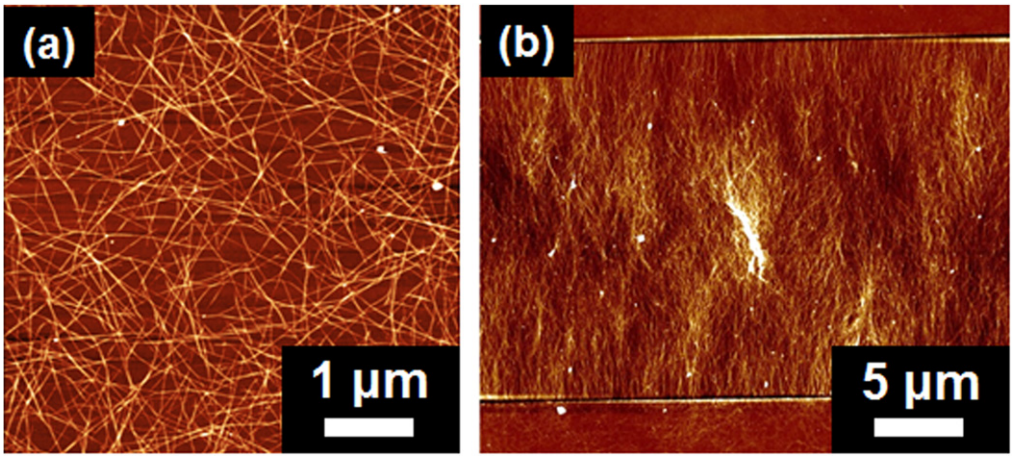

Figure 3. Atomic force microscopy images of (a) a random network of spin-coated SWNTs and (b) SWNTs aligned between two electrodes by application of a dc electric field (25 kV cm^{-1}) during drop-casting.

concentrations remain yet to be reached, and may not be economical. High resolution printing methods for low viscosity inks, such as inkjet printing (0.001–0.04 Pa s) and aerosol jet printing (0.001–1 Pa s) are much more suitable for the dilute carbon nanotube dispersions and have been applied numerous times to create devices and circuits [61, 97–109].

Many inks are water-based [101, 105] and the surfactants that stabilize the SWNT ink must be removed after printing by rinsing. At least on a lab scale, dispersions of surfactant-free SWNTs in organic solvents such as dimethylformamide (DMF) [98] or 1-cyclohexyl-2-pyrrolidone (CHP) [103] can be applied as well. Surface treatment (e.g. adhesion layers or UV-ozone treatment) and surface energy of the substrate also play an important role for printing of SWNTs [103, 108] and can be utilized to improve network density, alignment of the nanotubes or spatial resolution of the printing process [100, 110]. Once they are deposited, the strong adhesion of SWNTs to a suitable substrate allows for many layers of nanotubes to be printed on top of one another [101]. Thus, the density of SWNT networks can be tuned from just above the percolation threshold, for example for the channel of a transistor, to high density, for example, for injecting electrodes. Okimoto *et al* demonstrated the potential of this approach by fabricating all-carbon transistors using ink-jet printing of DMF-based SWNT dispersions [98].

Most of the mentioned deposition techniques, especially those that include slow drying processes and prior removal of dispersion stabilizers, will lead to SWNT bundles of various sizes. These may affect the transport properties of the networks [111]. In aligned networks thin bundles can improve the interconnectivity of the nanotubes, as the length of conformal contact between SWNTs is beneficial to charge transport along the bundle. However, thick and disordered bundles are likely to lead to non-uniform networks, limited overlap, insufficient electrostatic coupling in field-effect transistors and large barriers for charge transfer between bundles [112]. Additional carrier scattering that occurs in SWNT bundles [113] compared to pristine individual SWNTs reduces carrier mobility but is negligible compared to the junction-resistance [114] that dominates nanotube networks at least for channel lengths above 5 μm.

In comparison to other printable conducting and semiconducting materials such as PEDOT:PSS or conjugated polymers etc [115] carbon nanotube inks are more difficult to handle and their formulation and stabilization are critical. On the other hand, being able to print SWNT networks with different densities [98, 101] and of different types of carbon nanotubes offers the freedom to create devices with vastly different properties from the same material with excellent electronic and mechanical properties suitable for highly flexible, stretchable and transparent circuits.

5. SWNTs for electrodes

The high conductivity of metallic SWNTs, their low absorption cross section and mechanical flexibility have made carbon nanotubes a strong contender as a replacement for metals or transparent conductive oxides in flexible and stretchable electronics [116–118]. Early examples include the use of dense films of SWNTs as anodes in organic solar cells [119–122], light-emitting diodes [123, 124] and photodiodes [125]. For these applications it is not strictly necessary to use only metallic nanotubes if the films are dense enough. Doping with HNO_3 or $SOCl_2$ helps to increase the conductivity. Sheet resistances of a few hundred Ω/sq and less are readily achievable [80, 83, 126, 127]. However, in order to achieve higher transparency for similar sheet resistances, the semiconducting nanotubes should be removed [9]. The network conductance can be increased significantly when very long (several micrometers and longer) nanotubes are used in order to reduce the number of intertube junctions that exhibit resistances of hundreds of kΩ [114]. As most dispersion methods (ultrasonication/milling) cause more or less damage and shortening of the nanotubes [128], which decreases the conductivity of networks and composites, less damaging

methods are pursued. The dry deposition of nanotubes directly from growth in the gas phase onto filters and subsequent dry-transfer yields highly conductive and transparent networks as shown by Nasibulin *et al* [10]. A mild and scalable process to disperse carbon nanotubes without strong mechanical forces is their chemical reduction with sodium in liquid ammonia. The resulting nanotubide salt is soluble in dimethylsulfoxide and forms a nanotube ink that is stable at very high concentrations but is also highly air-sensitive [129]. After deposition, for example by spray coating or doctor-blading under inert atmosphere, the films are re-oxidized to the neutral species by exposure to dry air. Ostfeld *et al* demonstrated that for similar transparencies (80% at 550 nm) the sheet resistances of such films (about 60 Ω/sq) are lower compared to those produced by conventional SWNT dispersions in aqueous surfactant solutions (about 120 Ω/sq) [130]. Organic photovoltaic cells that were fabricated with these SWNT films and ITO as the transparent anode showed almost identical performance. It is evident that SWNT thin films have the potential to replace conducting oxides as materials for transparent electrodes, especially in areas where flexibility and stretchability are important. However, their relatively high cost and the question of uniformity over large areas, as well as possible hot-spots for leakage currents, must be addressed in the future.

Another interesting aspect for organic and flexible electronics is the application of carbon nanotubes as electrodes in organic field-effect transistors. Initially multi-walled and single-walled carbon nanotubes were added to conducting polymers such as PEDOT:PSS [132] and polyaniline [133] to increase the conductivity of these printable electrodes. Also, dense networks of SWNTs were used as injecting electrodes for both organic [134] and SWNT transistors [135, 136]. Schottky barriers and the resulting contact resistance between the semiconductor and the injecting electrode can be a limiting factor for the performance of organic FETs, in particular for n-type semiconductors that require low work function contacts [137]. Several studies have shown that SWNT electrodes or SWNT-decorated electrodes improve charge injection substantially and thus enhance device characteristics [134, 138–144]. Unlike other methods for increasing charge injection, such as modifying the work function of the injecting electrode, the enhancement of injection by carbon nanotubes is equal for holes and electrons. Figure 4 shows an example for the impact of carbon nanotubes on charge injection into organic semiconductors. Top-gate/bottom-contact transistors with the conjugated polymer F8BT as the semiconductor show ambipolar transport. However, due to the large mismatch of both HOMO and LUMO level (highest occupied molecular orbital and lowest unoccupied molecular orbital, respectively) with the work function of gold, the contact resistance is very high and non-ohmic when standard gold electrodes are used [145]. Coating these electrodes with a thin film of SWNTs substantially improved both hole and electron injection and consequently led to almost ohmic contacts and higher overall source-drain currents [131]. The underlying mechanism of injection improvement seems to be the strong electric field enhancement by the one-dimensional

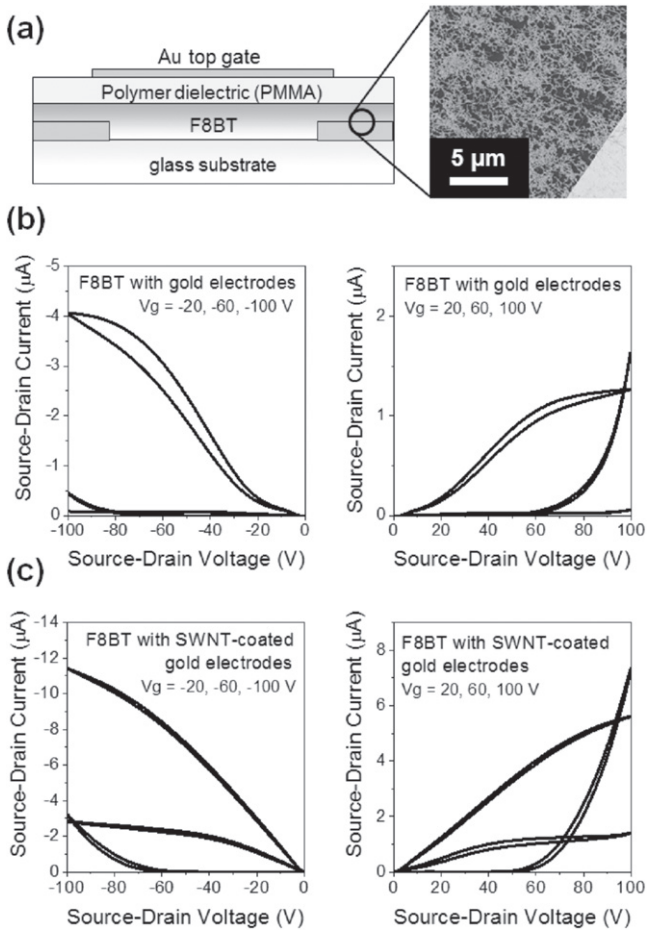

Figure 4. (a) Schematic illustration of a bottom-contact/top-gate polymer field-effect transistor with F8BT as the semiconductor. (b), (c) Ambipolar output characteristics of equivalent transistors with and without SWNT-coated gold electrodes [131].

carbon nanotubes. It is thus applicable to any organic semiconductor, and highlights the additional advantages of using SWNT electrodes in organic electronics.

An interesting combination of carbon nanotube networks and controlled modulation of charge carrier injection is used in vertical light-emitting field-effect transistors (VFET) as demonstrated by the Rinzler group [146–148]. Here a dense network of SWNTs is used as a semi-transparent, percolating source electrode separated by a thin dielectric layer from the gate electrode underneath. An organic semiconductor layer is sandwiched between the source electrode and a top drain electrode. The voltage applied to the gate electrode modulates the injection barrier between the source electrode and the organic semiconductor and enables switching behaviour, and thus an efficient combination of the drive transistor and the OLED in a display pixel [148]. This concept can also be applied to metallic mesh source electrodes [149, 150]. However, the nanotube network provides a nanoscale conducting mesh that is difficult to achieve by any other patterning method.

6. SWNT networks as semiconductors

While metallic carbon nanotubes are interesting as transparent electrodes for organic photovoltaic cells, as shown above, semiconducting SWNTs can also be used directly as the light-absorbing donor layer in heterojunction solar cells. As shown in figure 2(a), SWNTs absorb light in the near-infrared, which is advantageous for utilizing the whole solar spectrum for power generation [151, 152]. Their high carrier mobilities also promise to enable fast charge separation and transport to the electrodes, which is crucial for efficient solar cells [153]. Often C_{60} or PCBM serve as the electron acceptor layer in such photovoltaic cells [151, 154–156]. Again the purity of the semiconducting nanotube network is important, as metallic nanotubes would simply quench excitons and thus lower the efficiency. Energy transfer and charge trapping within a mix of semiconducting SWNTs would also result in a loss of power conversion efficiency. Unfortunately so far the maximum efficiency obtained in such solar cells is only 2.48% [157]. Given the high cost of the nanotube source material and purification, combined with the limited efficiency even compared to non-optimized organic bulk heterojunction solar cells (e.g. poly(3-hexylthiophene) with PCBM [158]), SWNT solar cells might be of more academic interest in terms of energy transfer and charge separation rather than their application.

More promising is the utilization of carbon nanotubes in field-effect transistors and electronic circuits. Individual semiconducting carbon nanotubes have been shown to be applicable in high performance circuits that can operate at high frequencies [159]. The extremely high charge carrier mobilities of individual nanotubes and their excellent electrostatic properties that enabled the fabrication of low voltage, sub 10 nm gate length transistors [160] continue to drive research in this area, although the initial promise of SWNTs as the solution to Moore's law [161] has not yet been fulfilled. For their application in printed and flexible electronics, however, the solution processability and flexibility of SWNT thin films instead of individual nanotubes combined with properties such as high carrier mobility and good on/off ratios will be most important.

For printed and flexible electronics, nanotubes will be used as random or semi-aligned networks, and transistor channel lengths will be large, i.e. a few micrometers or more. The density of nanotubes within the transistor channel must be at least above the percolation limit to allow for current flow. This limit depends on the length and alignment of the nanotubes. SWNT thin films can be modelled mathematically as a finite-sized tube percolation network with variable intertube coupling [162]. Ideally, densities are much higher than the percolation limit (>10 SWNT/μm) to ensure high on-conductance for a given channel width and length and thus high apparent mobility in a field-effect transistor. This becomes a problem when metallic nanotubes whose conductivity is not modulated by the gate field are still present. Depending on their percolation threshold, the off-currents of a given transistor can be very high [163] and can be reduced only slightly by 'striping' the SWNT film to disrupt the metallic pathways [164].

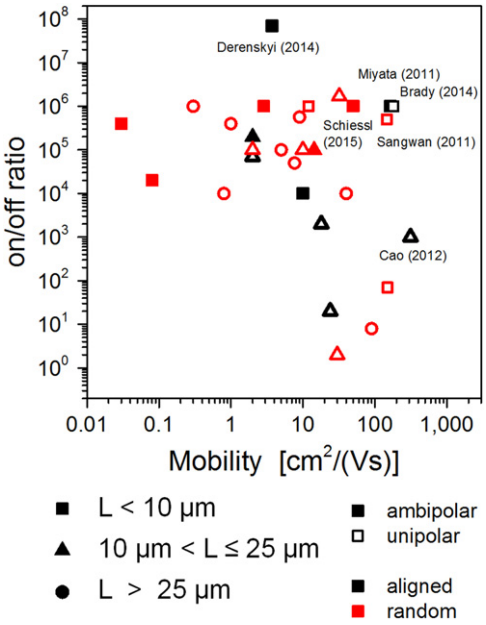

Figure 5. On/off ratio versus mobility performance map of FETs with solution-deposited, aligned and random SWNT networks, compiled from references [12, 50, 56, 63, 69, 77, 84, 86, 91, 95, 169–177].

The problem of residual metallic nanotubes led to a well-known trade-off between high on-conductance or apparent carrier mobility and high on/off current ratios [69, 165]. This is visualized in figure 5 where the on/off ratios are plotted versus the measured mobilities for a selection of solution-processed SWNT transistors that were published over the last few years. For possible applications of nanotube transistors in active-matrix OLED displays, the lower boundary for field-effect mobilities is 5–10 $cm^2\,V^{-1}\,s^{-1}$ [166]. At the same time the on/off current ratio should be at least 10^6 to avoid unnecessary power consumption and guarantee maximum brightness contrast for each pixel [167]. High on/off ratios (10^5–10^6) might be reached in SWNT network FETs despite the presence of residual metallic nanotubes but only for very sparse networks, which results in low on-conductances and low apparent mobilities (<1 $cm^2\,V^{-1}\,s^{-1}$) [168].

The on/off ratio can be improved for denser networks by increasing the channel length (>25 μm), thus making continuous metallic pathways less likely. This is demonstrated in figure 6 for random SWNT network transistors with long (40 μm) and short (5 μm) channel lengths and equal network densities with and without residual metallic SWNTs. For transistors with long channel lengths, the off-currents are almost the same, irrespective of the presence of metallic SWNTs. However, as the channel length decreases to 5 μm the residual metallic nanotubes can bridge the distance and the off-current increases by several orders of magnitude. For the transistor without metallic nanotubes, the off-current remains unchanged and only the on-current increases as expected [63]. Although longer channel lengths will give

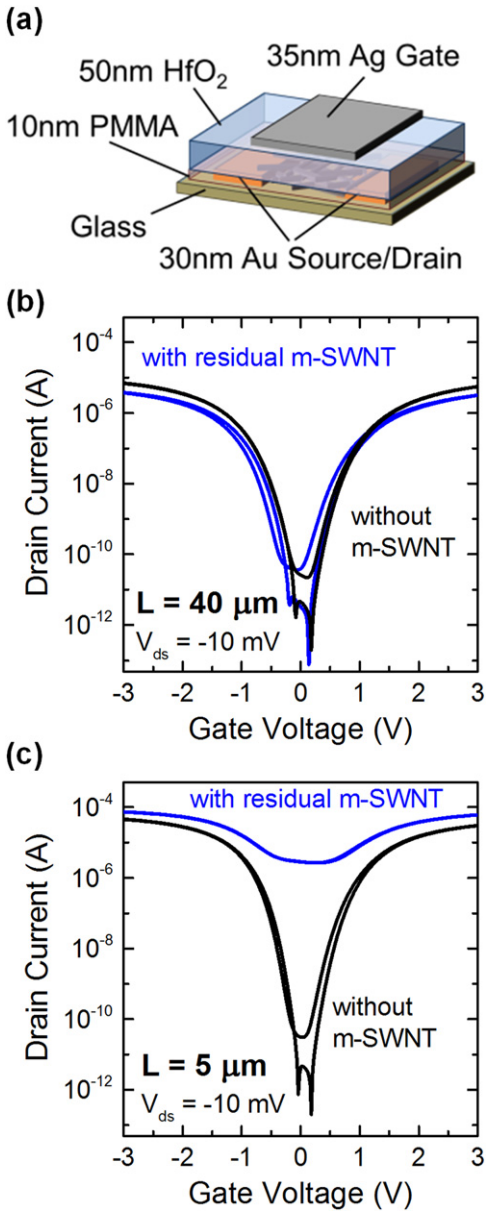

Figure 6. (a) Schematic illustration of bottom-contact/top-gate transistor with a spin-coated random network of sorted SWNTs and a PMMA/HfO_2 hybrid dielectric. (b) Ambipolar transfer characteristics of transistors with a long channel length of 40 μm with and without small amounts of residual metallic nanotubes. (b) Ambipolar transfer characteristics of transistors with a short channel length of 5 μm with and without small amounts of residual metallic nanotubes [63].

good on/off current ratios and high apparent mobilities for networks that contain some metallic SWNTs, the on-currents are lower compared to shorter channels and the overall transistor area increases, which is unfavourable for display pixels with current-driven OLEDs.

Clearly, the best way to reach maximum on-currents and minimum off-currents in a nanotube network transistor is to remove all metallic nanotubes. That is, more than 99% of SWNTs within the network must be semiconducting. Novel SWNT sorting methods such as gel-chromatography and selective polymer dispersion (see above) have recently enabled such pure semiconducting SWNT inks and thus a range of transistors and circuits with high mobilities (>100 $cm^2\,V^{-1}\,s^{-1}$) and high on/off ratios (10^6) even with submicrometer channel lengths were demonstrated [12, 176, 177].

The next question is, what type of semiconducting nanotube is best for FETs? The field-effect mobility of carbon nanotubes scales with the square of the diameter [5], thus large-diameter nanotubes would be preferable. However, their bandgap scales with the inverse of the diameter and has a direct impact on the off-current at least in short channel devices, so smaller diameter SWNTs with larger bandgaps would be better for higher on/off ratios [178]. Finally, the performance limiting factors are contact resistance [179] and tube–tube junctions [114, 180]. While the intertube junction resistance restricts the carrier transport within a dense network, the injection barriers at the metal contacts become limiting for shorter channels. As the channel resistance is reduced further and further, either by high nanotube densities or shorter channels, the contribution of the contact resistance increases. Even for moderately dense networks, the contact resistance can already be higher than the channel resistance [63]. A better understanding of charge injection into networks and charge transfer at nanotube junctions is necessary for further improvements in device performance.

As we have seen, the field-effect mobility of a semiconducting SWNT film is often cited as an important device parameter because it largely determines the switching speed and on-conductance of a transistor with a given geometry. In most cases, the carrier mobility in a field-effect transistor is calculated from the transconductance in the linear or saturation regime by taking into account the channel length L, width W, and the capacitance [181]. In a typical thin-film transistor the gate capacitance is based on the parallel plate capacitor model and calculated from the thickness and dielectric constant of the insulating layer. However, determining the effective capacitance for SWNT network devices is not as straightforward as for conventional thin film transistors. Due to the electrostatic coupling of the SWNTs with each other and thus screening of the gate field, in addition to the quantum capacitance of SWNTs ($C_Q = 4.0 \cdot 10^{-10}\,F\,m^{-1}$) [182], the usual plate–plate capacitor model (C_{PP}) can drastically overestimate the effective capacitance C_{eff}. For the calculation of the effective capacitance in a given device, the linear density of the SWNTs Λ_0^{-1}, the SWNT radius R, the effective dielectric thickness t and the relative permittivity ε_r of the dielectric must be taken into account as derived by Cao *et al* [183]:

$$C_{\text{eff}} = \Lambda_0^{-1} \cdot \left\{ C_Q^{-1} + 1/2\pi\varepsilon_0\varepsilon_r \ln\left[\Lambda_0/R\pi \cdot \sinh\left(2\pi t/\Lambda_0\right)\right] \right\}^{-1} \quad (1)$$

The difference between the effective and the plate–plate capacitance is large for low network densities of carbon nanotubes, as shown in figure 7. But even for high SWNT densities it should not be neglected, especially when the gate dielectric is very thin. While the effective capacitance for a

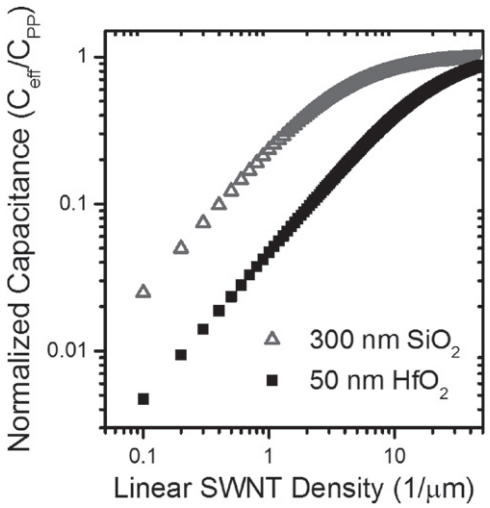

Figure 7. Illustration of the ratio between the effective capacitance (C_{eff}) as calculated according to equation (1) and the capacitance based on the parallel-plate model (C_{PP}) for different network densities and for two different types of gate dielectrics.

nanotube network with a linear density of about 5–10 μm^{-1} on a 300 nm thick SiO_2 dielectric is already very close to the calculated plate–plate capacitance, the same nanotube network on 50 nm of HfO_2 would result in an effective capacitance of only 20% to 40% of the C_{PP} value and thus lead to a large underestimation of the field-effect mobility. This calculation also implies that for very low SWNT densities (<1 μm^{-1}) decreasing the dielectric thickness much further, e.g. by using self-assembled monolayer dielectrics [177, 184, 185], will not increase the on-currents substantially. Thicker dielectrics may actually be more suitable in terms of device stability and breakdown voltages [135].

A serious problem of SWNT transistors has been their large current hysteresis and shift of threshold voltage, which would be a fatal deficiency for any application that requires bias stress stability, such as drive-transistors in OLED display pixels [166]. For p-type SWNT transistors a large threshold shift toward negative voltages is observed when they are operated in air. This effect has been largely attributed to the presence of water on hydrophilic substrates (e.g. oxides) and oxygen, which creates electron traps [186]. These also suppress electron transport in SWNTs under ambient conditions [187, 188]. The hysteresis is reduced and electron transport might be observed after devices are annealed in vacuum, covered with hydrophobic polymers (e.g. fluoropolymers) [189–191] or encapsulated with hybrid polymer/oxide films (see figure 6) [63].

SWNTs are intrinsically ambipolar with equal hole and electron mobilities (as shown in figure 6) although under ambient conditions they show a predominantly p-type behaviour [192]. For complementary circuits it is advantageous to have transistors that are either purely n-type or p-type but not ambipolar. Ambipolarity would lead to large power dissipation, for example, in complementary-like inverters. In order to create purely n-type SWNT transistors, molecular doping techniques have been applied, using polyethylene imine [193], viologen [194], NADH [195] and other reducing agents [174, 196]. The long term stability of these chemical dopants, especially under ambient conditions, remains to be tested. More permanent electrostatic n-doping is provided by encapsulation of nanotubes with PECVD-SiN_x, which contains fixed positive charges and results in robust n-type behaviour [197].

Overall, the device performance of SWNT network transistors has improved drastically over the last few years with field-effect mobilities and on/off ratios that are competitive with other solution-processable semiconductors. However, important parameters such as reproducibility, bias stress stability and control over doping still require further development.

7. Integrated circuits and applications

An impressive range of integrated circuits that use purified and sorted semiconducting carbon nanotubes has been demonstrated over the past few years. Transistors with good bias stress stability, high on/off ratios and high on-conductance might be used in OLED displays as switch and drive transistors in a simple 2T1C architecture [166, 167]. Here, the high carrier mobility of SWNT networks is a clear advantage over solution-processed organic semiconductors, which rarely reach carrier mobilities beyond 1–5 $cm^2 V^{-1} s^{-1}$ [198]. However, the sometimes still poor on/off ratios, threshold shifts under bias stress, and device-to-device variations for SWNT transistors are problematic. Nevertheless, several nanotube transistor driven single OLEDs [71, 78, 199, 200] and a small active-matrix display [201] were reported.

The requirements for transistors in active-matrix backplanes for sensing, e.g. pressure sensors or photodiode arrays, are less rigorous. Only one transistor is needed per pixel and the drive currents and bias stress are much lower. The inherent stretchability of SWNT networks is ideal for pressure sensing arrays that may need to be stretched over curved objects. Recent examples of backplanes based on SWNT FETs include flexible visible light/x-ray imagers [202], as well as conformal pressure and tactile sensor arrays [72, 203]. For such large area applications scalable and low-cost patterning methods are needed. Figure 8 shows the example of a 20×20 array of SWNT transistors that were patterned by gravure printing using silver nanoparticle ink for the electrodes and a barium titanate nanoparticle/poly(methyl methacrylate) composite for the gate dielectric [77]. The dielectric layer also served as an etch mask for the nanotubes, that were deposited by immersion of the PET substrate in a purified 99% semiconducting SWNT solution for two hours. The completed transistors showed mobilities of 4.3 ± 1.6 $cm^2 V^{-1} s^{-1}$ and on/off ratios of 10^4 to 10^5. The device-to-device variability was relatively high but still impressive for such a simple and low cost printing and patterning technique. Similar results were obtained by screen-printing of the same materials [78].

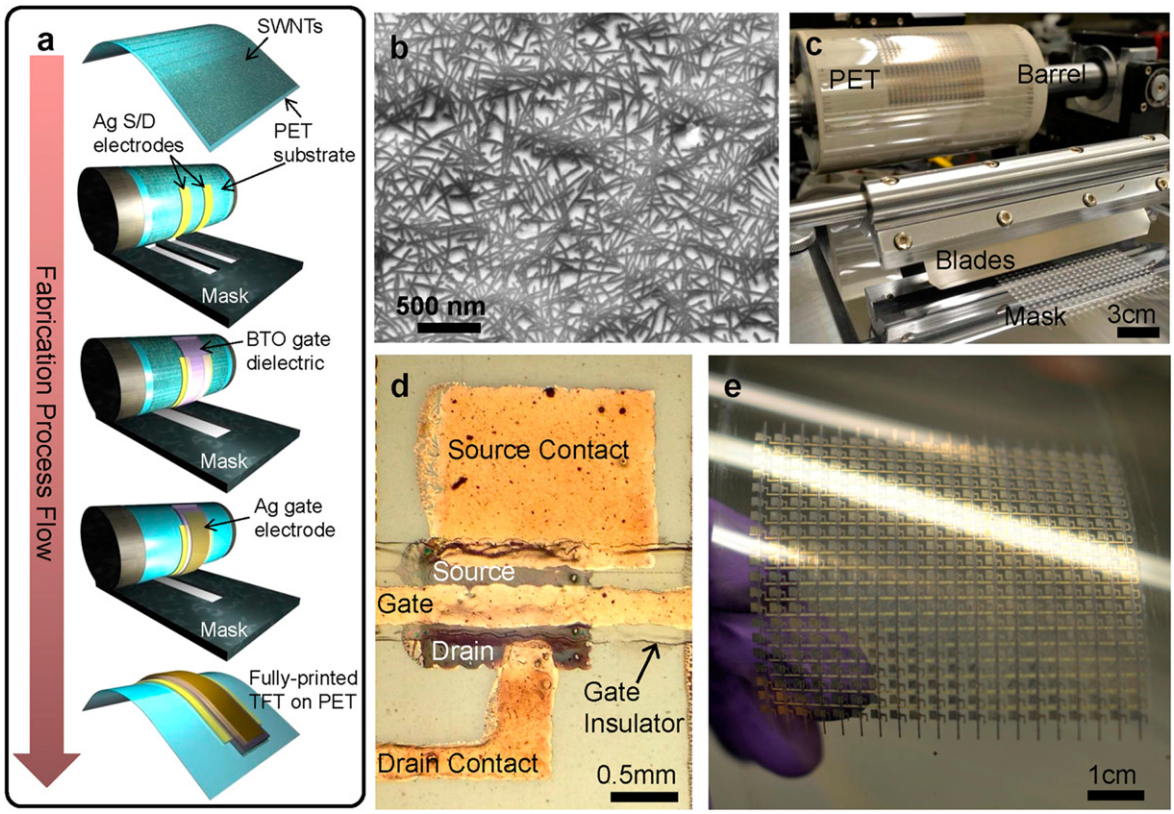

Figure 8. (a) Schematic of a SWNT deposition, patterning and printing process. (b) Scanning electron micrograph of a SWNT network deposited on a PET substrate. (c) Photograph of employed inverse gravure printer. (d) Optical micrograph of a single transistor, and (e) photograph of 20 × 20 device array on a PET substrate. Reprinted with permission from [77], copyright 2013, American Chemical Society.

Those printed transistor arrays on PET foil were flexible and bendable but not necessarily stretchable due to the mechanical limitations of the dielectric and the electrodes. In order to make full use of the excellent mechanical properties of SWNT networks, the other transistor components have to be optimized as well. A convenient way to enable stretchable SWNT transistors while maintaining high performance is the use of electrolyte-gating with soft or rubbery iongels [204, 205]. In an electrolyte-gated transistor the gate dielectric is replaced with an electrolyte, for example, an ionic liquid with a large electrochemical window [206]. When a gate voltage, and thus an electric field, is applied the anions and cations drift toward the gate electrode and the semiconductor, respectively, to form nm thick electric double layers. The applied gate voltage now drops across these thin double layers, which leads to very high effective capacitances on the order of 1–10 $\mu F\,cm^{-2}$. Hence, very high charge carrier densities can be accumulated at low gate voltages (<2 V). High on-conductances and low operating voltages are feasible [199, 207]. For networks of carbon nanotubes, electrolyte-gating is especially efficient and avoids the problem of tube-to-tube screening as the ions accumulate around each nanotube. The effective capacitance is only limited by the quantum capacitance of the carbon nanotubes [182, 208, 209]. The main drawback of electrolyte-gating is the limitation of the switching speed by the movement of the ions in the electrolyte, although the maximum operating frequencies of electrolyte-gated SWNT transistors are still in the MHz range [106].

Iongels are printable and flexible and combine the high ionic mobility of ionic liquids with the mechanical stability of polymer gels. They have been shown to be highly suitable for various electrolyte-gated transistors [210–213] including SWNT transistors [105]. Xu *et al* used purified (7, 5) SWNT networks, pre-stretched buckled gold electrodes and an iongel to create highly stretchable transistors on a PDMS substrate [204]. The devices could be strained up to 18% before the on-currents started to drop. Further, combining metallic SWNT electrodes with semiconducting SWNT networks for metal-free all-carbon transistors could provide excellent flexibility and stretchability as well as transparency as recently demonstrated by Sun *et al* with dry-transferred CVD-grown SWNT networks [135].

While individual transistors can be used to study charge transport in solution-processed or printed SWNT networks, more complex circuit structures and more rigorous requirements on switching speed and device-to-device uniformity are necessary for future SWNT-based electronics. Basic integrated circuits have already been fabricated using solution-processed SWNT networks such as complementary inverters [63, 108, 174, 194, 197, 214, 215], ring-oscillators which consist of an uneven number of connected inverters [105, 106, 109, 191, 216, 217], NAND gates [174, 214, 218], NOR gates [109], D-Flip-Flops [219, 220] and others. These

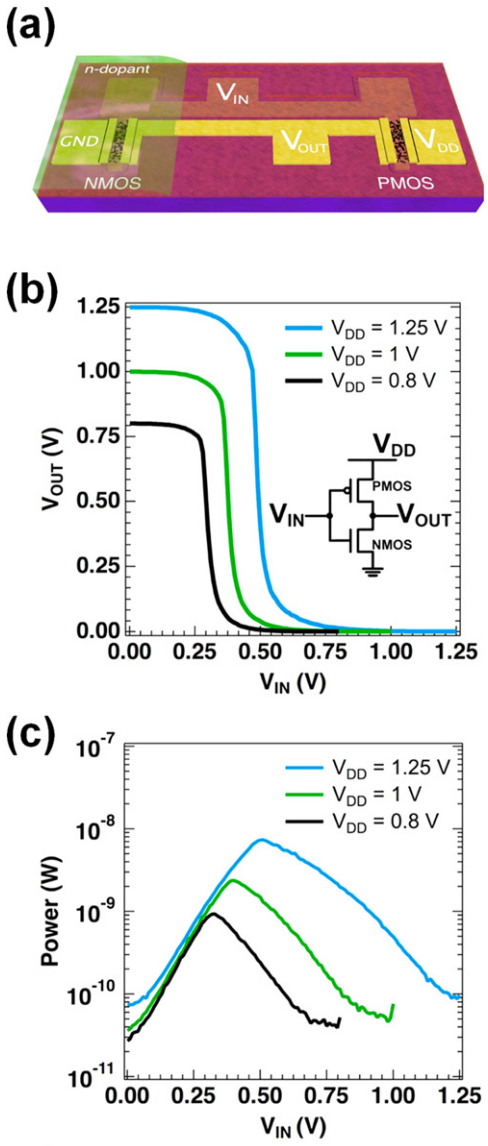

Figure 9. (a) Schematic illustration of an SWNT inverter with doped n-type (NMOS) and p-type (PMOS) transistors. (b) Voltage transfer curves (inset shows the circuit diagram of the inverter). (c) Power characteristics of the inverter during operation. (a) and (b) reprinted with permission from [214], copyright 2013, American Chemical Society.

circuits are the basis for even more complex devices such as RF-ID tags [221], static random access memories (SRAM) [135], shift registers, and so on.

As one of the fundamental building blocks for integrated circuits, the inverter is a good example to illustrate the requirements and challenges for SWNT circuits. The most common inverter design is that of a complementary inverter consisting of an n-type and a p-type transistor in series and connected gate electrodes as the input node (see inset, figure 9). At a given low or high input voltage one transistor is on and the other is off. Consequently, the output voltage is high and close to the supply voltage (V_{DD}) or very low (~0 V), respectively (see figure 9(b)). The on-currents and threshold voltages of the two transistors must be matched to obtain rail-to-rail operation, that is, full inversion of the input voltage. The complementary inverter design provides high gain and a large noise margin, which is essential for the successful integration of a large number of inverters. Power dissipation is low because current only flows at the inversion point (see figure 9(c)), that is, only for short periods of time.

Unfortunately, under ambient conditions SWNT network transistors exhibit mainly hole transport as mentioned above. In order to create stable n-type behaviour local doping is required (see above and figure 9) [194, 214]. An alternative to n-doping of the SWNT network is the incorporation of other solution-processable, high-mobility semiconductors such as zinc tin oxide for n-type transistors in combination with SWNT p-type transistors [222]. Good control over the threshold voltages is also needed in order to achieve voltage inversion ideally at half of the supply voltage. On/off ratios of the individual transistors must be high even at high source-drain voltages (i.e. supply voltage).

Ambipolar SWNT transistors can be employed to create complementary-like inverters that are usable for MHz ring-oscillators [63, 106, 109]. Here, only one semiconducting layer is necessary and under ideal conditions the hole and electron mobilities are equal. However, since none of the transistors can be fully off at any input voltage, the static current flow and thus power dissipation in ambipolar inverters is very high. Truly complementary SWNT inverters are superior in performance but require more processing, which may lead to device-to-device variations and patterning problems at higher integration densities.

Despite these challenges the fabrication of short channel (<200 nm) transistors with very dense and aligned semiconducting SWNT arrays from sorted dispersions exhibiting on-conductances of $197 \pm 38\ \mu S\ \mu m^{-1}$ and on/off ratios of 10^5 by Brady *et al* [176] has again strengthened the endeavour to create high-performance, low power SWNT thin-film electronics for a post-silicon era. For given parameters, SWNT transistors could indeed outperform silicon FinFETs in terms of energy consumption and speed [16]. The numerous examples of integrated SWNT thin film circuits and the recent demonstration of a rudimentary SWNT computer based on aligned chemical vapor deposition (CVD) grown SWNTs emphasize the high potential for future carbon nanotube electronics whose full realization has finally become tangible [223].

A novel and somewhat unusual application of semiconducting SWNTs is as nanoscale emitters in near-infrared light-emitting devices. Light emission from semiconducting SWNTs can originate either from the impact excitation of accelerated holes or electrons [224–226] or electron-hole recombination [91, 227, 228]. Unfortunately, SWNTs are not particularly good emitters. Their quantum efficiencies reach a few percent at best and depend somewhat on chirality [229]. This deficiency has been attributed to the high mobility of excitons along the nanotubes, which enables them to find quenching sites, such as the tube ends or other defects, very quickly [230, 231]. However, for a single nanotube species the photoluminescence line width at room temperature is very narrow (<40 meV) [232] and directly determined by its chirality with some influence by the surrounding dielectric

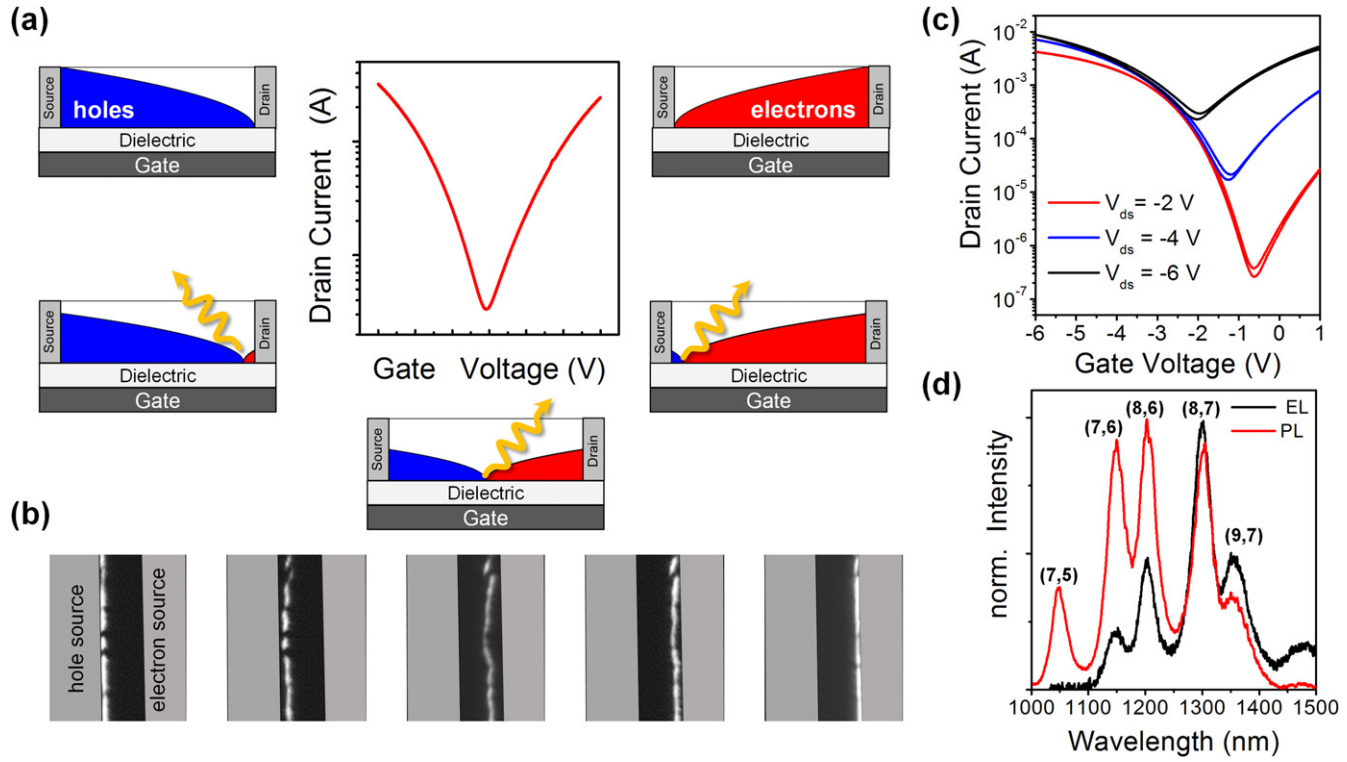

Figure 10. (a) Schematic illustration of the spatial distribution of holes and electrons in an ambipolar field-effect transistor for different gate voltages. (b) Near-infrared emission images of an ambipolar SWNT network transistor for different gate voltages showing movement of the emission zone through the channel (channel length 20 μm). (c) Ambipolar transfer characteristics of an SWNT network transistor with five semiconducting nanotubes species. (d) Electroluminescence and photoluminescence spectra of this transistor indicate increased emission from narrow bandgap SWNTs.

[233]. Their emission wavelengths between 900 nm and 2000 nm make them interesting for biological imaging [234, 235] and as nanoscale light sources for on-chip optical communication [236–238].

So far, there have been no examples of light-emitting diodes based on s-SWNTs in a conventional vertical stack structure. It is, however, possible to create a p-i-n-junction in a single nanotube or an array of SWNTs by employing two oppositely biased gates in a transistor structure. A clear rectifying behaviour and light-emission can be observed that originates from electron–hole recombination [239, 240]. Due to the intrinsic ambipolar transport in un-doped SWNT networks the simultaneous accumulation of holes and electrons within the channel is also easily achieved with a single gate electrode. When the gate voltage is set between the source voltage (usually at ground, 0 V) and the drain voltage, the effective gate potential is positive with respect to one electrode and negative for the other. Thus, a hole and an electron accumulation layer form. The lateral extent of the two accumulation layers and hence their meeting point depends on the gate and drain voltages. The resulting narrow emission zone can be moved through the entire channel, as shown in figures 10(a) and (b), by simply changing the applied bias. This is a typical property of all ambipolar transistors based on emissive semiconductors such as conjugated polymers [145] or quantum dots [241], and also works for a single carbon nanotube [227, 242].

For ambipolar networks of different semiconducting nanotubes, the electroluminescence spectrum of such a light-emitting transistor exhibits emission peaks at the same wavelengths and with the same line width as the corresponding photoluminescence spectrum. However, the intensity distribution is shifted toward nanotubes with smaller bandgaps [89] as shown in figure 10(d). Further, at very high charge carrier densities that can be achieved by electrolyte-gating [89] the electroluminescence spectrum shows additional peaks [90] that can be attributed to emission from charged excitons, i.e. trions [243, 244].

Light-emitting SWNT devices based on impact excitation are usually unipolar and require high lateral electric fields to provide the necessary kinetic energy to create excitons [224, 226, 245, 246]. In order to keep voltages low the distance between the electrodes must be short (<1 μm), gate electrodes are not necessary if carrier injection is sufficient [247, 248]. Since the created excitons are not fully thermalized before photon emission the electroluminescence spectra of these devices are significantly broadened (peak width 100–200 meV) [249]. Due to the high excitation energies even E_{22} emission appears to be possible [250].

Although the emission efficiencies for both types of SWNT light-emitting devices are very low and reach 0.01% at maximum, the large current densities enable reasonable optical output and the emitted light is strongly polarized [90, 240]. The possibility to couple these planar and tuneable

near-infrared emitters to waveguides [238] on a chip could lead to interesting applications of SWNTs beyond simple electronic circuits.

8. Conclusions

Over the last few years the field of solution-processed carbon nanotube electronics has made tremendous progress. One of the major problems that prevented the application of carbon nanotubes as semiconductors in printable and flexible electronics—the separation of metallic and semiconducting nanotubes—has finally been solved. Dispersions of purely semiconducting nanotubes can be produced economically on a large scale. This finally allows the numerous excellent properties of carbon nanotube networks to be utilized in large area, printed, flexible and stretchable electronic devices. Although there are still a number of challenges that need to be addressed, for example stable n-doping, bias stress stability, uniformity, etc, the opportunities of carbon nanotube-based devices are plentiful and many impressive examples already exist. In addition to the engineering task of creating functioning prototypes, future fundamental research could focus on the peculiarities of charge transport in networks of carbon nanotubes with different bandgaps and different densities beyond simple percolation theory. Long term performance stability under ambient conditions and the influence of bias and mechanical stress will be of interest, as well as light emission from SWNT networks. Overall, the field of carbon nanotube electronics has finally entered a phase where, thanks to the availability of pure and well-defined materials, much more reliable structure–property relationships can be investigated and exploited, and real-world applications become feasible.

Acknowledgments

The author thanks Stefan P Schießl, Marcel Rother and Florian Jakubka for help with preparing figures and literature search. This work was supported by the European Research Council under the European Union's Seventh Framework Programme (FP/2007-2013) / ERC Grant Agreement No. 306298 (EN-LUMINATE).

References

[1] Yao Z, Kane C L and Dekker C 2000 High-field electrical transport in single-wall carbon nanotubes *Phys. Rev. Lett.* **84** 2941–4
[2] Dai H, Wong E W and Lieber C M 1996 Probing electrical transport in nanomaterials: conductivity of individual carbon nanotubes *Science* **272** 523–6
[3] Martel R, Derycke V, Lavoie C, Appenzeller J, Chan K K, Tersoff J and Avouris P 2001 Ambipolar electrical transport in semiconducting single-wall carbon nanotubes *Phys. Rev. Lett.* **87** 256805
[4] Lin Y M, Appenzeller J and Avouris P 2004 Ambipolar-to-unipolar conversion of carbon nanotube transistors by gate structure engineering *Nano Lett.* **4** 947–50
[5] Zhou X J, Park J Y, Huang S M, Liu J and McEuen P L 2005 Band structure, phonon scattering, and the performance limit of single-walled carbon nanotube transistors *Phys. Rev. Lett.* **95** 146805
[6] Durkop T, Getty S A, Cobas E and Fuhrer M S 2004 Extraordinary mobility in semiconducting carbon nanotubes *Nano Lett.* **4** 35–9
[7] Ruoff R S, Qian D and Liu W K 2003 Mechanical properties of carbon nanotubes: theoretical predictions and experimental measurements *C. R. Physique* **4** 993–1008
[8] Sekitani T, Nakajima H, Maeda H, Fukushima T, Aida T, Hata K and Someya T 2009 Stretchable active-matrix organic light-emitting diode display using printable elastic conductors *Nat. Mater.* **8** 494–9
[9] Green A A and Hersam M C 2008 Colored semitransparent conductive coatings consisting of monodisperse metallic single-walled carbon nanotubes *Nano Lett.* **8** 1417–22
[10] Nasibulin A G *et al* 2011 Multifunctional free-standing single-walled carbon nanotube films *ACS Nano* **5** 3214–21
[11] Sangwan V K, Ortiz R P, Alaboson J M P, Emery J D, Bedzyk M J, Lauhon L J, Marks T J and Hersam M C 2012 Fundamental performance limits of carbon nanotube thin-film transistors achieved using hybrid molecular dielectrics *ACS Nano* **6** 7480–8
[12] Miyata Y, Shiozawa K, Asada Y, Ohno Y, Kitaura R, Mizutani T and Shinohara H 2011 Length-sorted semiconducting carbon nanotubes for high-mobility thin film transistors *Nano Res.* **4** 963–70
[13] Chen Y, Zhang Y, Hu Y, Kang L, Zhang S, Xie H, Liu D, Zhao Q, Li Q and Zhang J 2014 State of the art of single-walled carbon nanotube synthesis on surfaces *Adv. Mater.* **26** 5898–922
[14] Wang C, Takei K, Takahashi T and Javey A 2013 Carbon nanotube electronics—moving forward *Chem. Soc. Rev.* **42** 2592–609
[15] Jariwala D, Sangwan V K, Lauhon L J, Marks T J and Hersam M C 2013 Carbon nanomaterials for electronics, optoelectronics, photovoltaics, and sensing *Chem. Soc. Rev.* **42** 2824–60
[16] Tulevski G S, Franklin A D, Frank D, Lobez J M, Cao Q, Park H, Afzali A, Han S-J, Hannon J B and Haensch W 2014 Toward high-performance digital logic technology with carbon nanotubes *ACS Nano* **8** 8730–45
[17] Sun D-M, Liu C, Ren W-C and Cheng H-M 2013 A review of carbon nanotube- and graphene-based flexible thin-film transistors *Small* **9** 1188–205
[18] Wong H-S P and Akinwande D 2011 *Carbon Nanotube and Graphene Device Physics* (Cambridge: Cambridge University Press)
[19] Charlier J C, Blase X and Roche S 2007 Electronic and transport properties of nanotubes *Rev. Mod. Phys.* **79** 677–732
[20] Ilani S and McEuen P L 2010 Electron transport in carbon nanotubes *Annu. Rev. Condens. Matter Phys.* **1** 1–25
[21] Bachilo S M, Strano M S, Kittrell C, Hauge R H, Smalley R E and Weisman R B 2002 Structure-assigned optical spectra of single-walled carbon nanotubes *Science* **298** 2361–6
[22] Kataura H, Kumazawa Y, Maniwa Y, Umezu I, Suzuki S, Ohtsuka Y and Achiba Y 1999 Optical properties of single-wall carbon nanotubes *Synth. Met.* **103** 2555–8
[23] Weisman R B and Bachilo S M 2003 Dependence of optical transition energies on structure for single-walled carbon nanotubes in aqueous suspension: an empirical Kataura plot *Nano Lett.* **3** 1235–8

[24] Jorio A, Pimenta M A, Souza A G, Saito R, Dresselhaus G and Dresselhaus M S 2003 Characterizing carbon nanotube samples with resonance Raman scattering *New J. Phys.* **5** 1–17
[25] Nikolaev P, Bronikowski M J, Bradley R K, Rohmund F, Colbert D T, Smith K A and Smalley R E 1999 Gas-phase catalytic growth of single-walled carbon nanotubes from carbon monoxide *Chem. Phys. Lett.* **313** 91–7
[26] Lolli G, Zhang L A, Balzano L, Sakulchaicharoen N, Tan Y Q and Resasco D E 2006 Tailoring (n,m) structure of single-walled carbon nanotubes by modifying reaction conditions and the nature of the support of CoMo catalysts *J. Phys. Chem.* B **110** 2108–15
[27] Journet C, Maser W K, Bernier P, Loiseau A, de la Chapelle M L, Lefrant S, Deniard P, Lee R and Fischer J E 1997 Large-scale production of single-walled carbon nanotubes by the electric-arc technique *Nature* **388** 756–8
[28] Guo T, Nikolaev P, Thess A, Colbert D T and Smalley R E 1995 Catalytic growth of single-walled manotubes by laser vaporization *Chem. Phys. Lett.* **243** 49–54
[29] Ando Y, Zhao X, Hirahara K, Suenaga K, Bandow S and Iijima S 2000 Mass production of single-wall carbon nanotubes by the arc plasma jet method *Chem. Phys. Lett.* **323** 580–5
[30] Kim K S, Cota-Sanchez G, Kingston C T, Imris M, Simard B and Soucy G 2007 Large-scale production of single-walled carbon nanotubes by induction thermal plasma *J. Phys. D: Appl. Phys.* **40** 2375
[31] Kim K S, Kingston C T, Ruth D, Barnes M and Simard B 2014 Synthesis of high quality single-walled carbon nanotubes with purity enhancement and diameter control by liquid precursor Ar–H2 plasma spraying *Chem. Eng.* J **250** 331–41
[32] Bergin S D *et al* 2008 Towards solutions of single-walled carbon nanotubes in common solvents *Adv. Mater.* **20** 1876–81
[33] Coleman J N 2009 Liquid-phase exfoliation of nanotubes and graphene *Adv. Funct. Mater.* **19** 3680–95
[34] O'Connell M J *et al* 2002 Band gap fluorescence from individual single-walled carbon nanotubes *Science* **297** 593–6
[35] McDonald T J, Engtrakul C, Jones M, Rumbles G and Heben M J 2006 Kinetics of PL quenching during single-walled carbon nanotube rebundling and diameter-dependent surfactant interactions *J. Phys. Chem.* B **110** 25339–46
[36] Nakashima N, Okuzono S, Murakami H, Nakai T and Yoshikawa K 2003 DNA dissolves single-walled carbon nanotubes in water *Chem. Lett.* **32** 456–7
[37] Zheng M, Jagota A, Semke E D, Diner B A, McLean R S, Lustig S R, Richardson R E and Tassi N G 2003 DNA-assisted dispersion and separation of carbon nanotubes *Nat. Mater.* **2** 338–42
[38] Zheng M *et al* 2003 Structure-based carbon nanotube sorting by sequence-dependent DNA assembly *Science* **302** 1545–8
[39] Tu X M, Manohar S, Jagota A and Zheng M 2009 DNA sequence motifs for structure-specific recognition and separation of carbon nanotubes *Nature* **460** 250–3
[40] Arnold M S, Stupp S I and Hersam M C 2005 Enrichment of single-walled carbon nanotubes by diameter in density gradients *Nano Lett.* **5** 713–8
[41] Arnold M S, Green A A, Hulvat J F, Stupp S I and Hersam M C 2006 Sorting carbon nanotubes by electronic structure using density differentiation *Nat. Nanotechnol.* **1** 60–5
[42] Liu H, Nishide D, Tanaka T and Kataura H 2011 Large-scale single-chirality separation of single-wall carbon nanotubes by simple gel chromatography *Nat. Commun.* **2** 309
[43] Tanaka T, Liu H, Fujii S and Kataura H 2011 From metal/semiconductor separation to single-chirality separation of single-wall carbon nanotubes using gel *Physica Status Solidi RRL* **5** 301–6
[44] Tulevski G S, Franklin A D and Afzali A 2013 High purity isolation and quantification of semiconducting carbon nanotubes via column chromatography *ACS Nano* **7** 2971–6
[45] Flavel B S, Moore K E, Pfohl M, Kappes M M and Hennrich F 2014 Separation of single-walled carbon nanotubes with a gel permeation chromatography system *ACS Nano* **8** 1817–26
[46] Hirano A, Tanaka T and Kataura H 2012 Thermodynamic determination of the metal/semiconductor separation of carbon nanotubes using hydrogels *ACS Nano* **6** 10195–205
[47] Liu H, Tanaka T, Urabe Y and Kataura H 2013 High-efficiency single-chirality separation of carbon nanotubes using temperature-controlled gel chromatography *Nano Lett.* **13** 1996–2003
[48] Nish A, Hwang J Y, Doig J and Nicholas R J 2007 Highly selective dispersion of singlewalled carbon nanotubes using aromatic polymers *Nat. Nanotechnol.* **2** 640–6
[49] Chen F M, Wang B, Chen Y and Li L J 2007 Toward the extraction of single species of sinale-walled carbon nanotubes using fluorene-based polymers *Nano Lett.* **7** 3013–7
[50] Gomulya W *et al* 2013 Semiconducting single-walled carbon nanotubes on demand by polymer wrapping *Adv. Mater.* **25** 2948–56
[51] Berton N, Lemasson F, Tittmann J, Stürzl N, Hennrich F, Kappes M M and Mayor M 2011 Copolymer-controlled diameter-selective dispersion of semiconducting single-walled carbon nanotubes *Chem. Mat.* **23** 2237–49
[52] Mistry K S, Larsen B A and Blackburn J L 2013 High-yield dispersions of large-diameter semiconducting single-walled carbon nanotubes with tunable narrow chirality distributions *ACS Nano* **7** 2231–9
[53] Tange M, Okazaki T and Iijima S 2012 Selective extraction of semiconducting single-wall carbon nanotubes by poly(9, 9-dioctylfluorene-alt-pyridine) for 1.5 μm emission *ACS Appl. Mater. Interfaces* **4** 6458–62
[54] Ozawa H, Ide N, Fujigaya T, Niidome Y and Nakashima N 2011 One-pot separation of highly enriched (6, 5)-single-walled carbon nanotubes using a fluorene-based copolymer *Chem. Lett.* **40** 239–41
[55] Ozawa H, Fujigaya T, Niidome Y, Hotta N, Fujiki M and Nakashima N 2011 Rational concept to recognize/extract single-walled carbon nanotubes with a specific chirality *J. Am. Chem. Soc.* **133** 2651–7
[56] Lee H W *et al* 2011 Selective dispersion of high purity semiconducting single-walled carbon nanotubes with regioregular poly(3-alkylthiophene)s *Nat. Commun.* **2** 541
[57] Wang H, Koleilat G I, Liu P, Jiménez-Osés G, Lai Y-C, Vosgueritchian M, Fang Y, Park S, Houk K N and Bao Z 2014 High-yield sorting of small-diameter carbon nanotubes for solar cells and transistors *ACS Nano* **8** 2609–17
[58] Lemasson F, Berton N, Tittmann J, Hennrich F, Kappes M M and Mayor M 2011 Polymer library comprising fluorene and carbazole homo- and copolymers for selective single-walled carbon nanotubes extraction *Macromolecules* **45** 713–22
[59] Lemasson F A, Strunk T, Gerstel P, Hennrich F, Lebedkin S, Barner-Kowollik C, Wenzel W, Kappes M M and Mayor M 2011 Selective dispersion of single-walled carbon nanotubes with specific chiral indices by poly(N-decyl-2, 7-carbazole) *J. Am. Chem. Soc.* **133** 652–5
[60] Hwang J Y, Nish A, Doig J, Douven S, Chen C W, Chen L C and Nicholas R J 2008 Polymer structure and solvent effects on the selective dispersion of single-walled carbon nanotubes *J. Am. Chem. Soc.* **130** 3543–53

[61] Wang H, Hsieh B, Jiménez-Osés G, Liu P, Tassone C J, Diao Y, Lei T, Houk K N and Bao Z 2015 Solvent effects on polymer sorting of carbon nanotubes with applications in printed electronics *Small* **11** 126–33
[62] Jakubka F, Schießl S P, Martin S, Englert J M, Hauke F, Hirsch A and Zaumseil J 2012 Effect of polymer molecular weight and solution parameters on selective dispersion of single-walled carbon nanotubes *ACS Macro Lett.* **1** 815–9
[63] Schießl S P, Fröhlich N, Held M, Gannott F, Schweiger M, Forster M, Scherf U and Zaumseil J 2015 Polymer-sorted semiconducting carbon nanotube networks for high-performance ambipolar field-effect transistors *ACS Appl. Mater. Interfaces* **7** 682–9
[64] Berton N, Lemasson F, Hennrich F, Kappes M M and Mayor M 2012 Influence of molecular weight on selective oligomer-assisted dispersion of single-walled carbon nanotubes and subsequent polymer exchange *Chem. Comm.* **48** 2516–8
[65] Wang W Z, Li W F, Pan X Y, Li C M, Li L-J, Mu Y G, Rogers J A and Chan-Park M B 2011 Degradable conjugated polymers: synthesis and applications in enrichment of semiconducting single-walled carbon nanotubes *Adv. Funct. Mater.* **21** 1643–51
[66] Toshimitsu F and Nakashima N 2014 Semiconducting single-walled carbon nanotubes sorting with a removable solubilizer based on dynamic supramolecular coordination chemistry *Nat. Commun.* **5** 5041
[67] Liang S, Zhao Y and Adronov A 2013 Selective and reversible noncovalent functionalization of single-walled carbon nanotubes by a pH-responsive vinylogous tetrathiafulvalene–fluorene copolymer *J. Am. Chem. Soc.* **136** 970–7
[68] Samanta S K, Fritsch M, Scherf U, Gomulya W, Bisri S Z and Loi M A 2014 Conjugated polymer-assisted dispersion of single-wall carbon nanotubes: the power of polymer wrapping *Acc. Chem. Res.* **47** 2446–56
[69] Rouhi N, Jain D, Zand K and Burke P J 2011 Fundamental limits on the mobility of nanotube-based semiconducting inks *Adv. Mater.* **23** 94–9
[70] Roberts M E, LeMieux M C, Sokolov A N and Bao Z N 2009 Self-sorted nanotube networks on polymer dielectrics for low-voltage thin-film transistors *Nano Lett.* **9** 2526–31
[71] Wang C, Zhang J, Ryu K, Badmaev A, De Arco L G and Zhou C 2009 Wafer-scale fabrication of separated carbon nanotube thin-film transistors for display applications *Nano Lett.* **9** 4285–91
[72] Takahashi T, Takei K, Gillies A G, Fearing R S and Javey A 2011 Carbon nanotube active-matrix backplanes for conformal electronics and sensors *Nano Lett.* **11** 5408–13
[73] Wang C, Chien J-C, Takei K, Takahashi T, Nah J, Niknejad A M and Javey A 2012 Extremely bendable, high-performance integrated circuits using semiconducting carbon nanotube networks for digital, analog, and radio-frequency applications *Nano Lett.* **12** 1527–33
[74] Zhang Q, Vichchulada P and Lay M D 2010 Length, bundle, and density gradients in spin cast single-walled carbon nanotube networks *J. Phys. Chem.* C **114** 16292–7
[75] Liyanage L S, Lee H, Patil N, Park S, Mitra S, Bao Z and Wong H-S P 2011 Wafer-scale fabrication and characterization of thin-film transistors with polythiophene-sorted semiconducting carbon nanotube networks *ACS Nano* **6** 451–8
[76] Kiriya D, Chen K, Ota H, Lin Y, Zhao P, Yu Z, Ha T-J and Javey A 2014 Design of surfactant–substrate interactions for roll-to-roll assembly of carbon nanotubes for thin-film transistors *J. Am. Chem. Soc.* **136** 11188–94
[77] Lau P H, Takei K, Wang C, Ju Y, Kim J, Yu Z, Takahashi T, Cho G and Javey A 2013 Fully printed, high performance carbon nanotube thin-film transistors on flexible substrates *Nano Lett.* **13** 3864–9
[78] Cao X, Chen H, Gu X, Liu B, Wang W, Cao Y, Wu F and Zhou C 2014 Screen printing as a scalable and low-cost approach for rigid and flexible thin-film transistors using separated carbon nanotubes *ACS Nano* **8** 12769–76
[79] Liu Z, Li H, Qiu Z, Zhang S-L and Zhang Z-B 2012 SMALL-hysteresis thin-film transistors achieved by facile dip-coating of nanotube/polymer composite *Adv. Mater.* **24** 3633–8
[80] Mirri F, Ma A W K, Hsu T T, Behabtu N, Eichmann S L, Young C C, Tsentalovich D E and Pasquali M 2012 High-performance carbon nanotube transparent conductive films by scalable dip coating *ACS Nano* **6** 9737–44
[81] Tenent R C, Barnes T M, Bergeson J D, Ferguson A J, To B, Gedvilas L M, Heben M J and Blackburn J L 2009 Ultrasmooth, large-area, high-uniformity, conductive transparent single-walled-carbon-nanotube films for photovoltaics produced by ultrasonic spraying *Adv. Mater.* **21** 3210–6
[82] Liu Q, Fujigaya T, Cheng H-M and Nakashima N 2010 Free-standing highly conductive transparent ultrathin single-walled carbon nanotube films *J. Am. Chem. Soc.* **132** 16581–6
[83] Dan B, Irvin G C and Pasquali M 2009 Continuous and scalable fabrication of transparent conducting carbon nanotube films *ACS Nano* **3** 835–43
[84] Derenskyi V *et al* 2014 Carbon nanotube network ambipolar field-effect transistors with 108 on/off ratio *Adv. Mater.* **26** 5969–75
[85] Krupke R, Hennrich F, von Lohneysen H and Kappes M M 2003 Separation of metallic from semiconducting single-walled carbon nanotubes *Science* **301** 344–7
[86] Izard N, Kazaoui S, Hata K, Okazaki T, Saito T, Iijima S and Minami N 2008 Semiconductor-enriched single wall carbon nanotube networks applied to field effect transistors *Appl. Phys. Lett.* **92** Art.No.243112
[87] Shekhar S, Stokes P and Khondaker S I 2011 Ultrahigh density alignment of carbon nanotube arrays by dielectrophoresis *ACS Nano* **5** 1739–46
[88] Stokes P, Silbar E, Zayas Y M and Khondaker S I 2009 Solution processed large area field effect transistors from dielectrophoreticly aligned arrays of carbon nanotubes *Appl. Phys. Lett.* **94** 113104
[89] Grimm S B, Jakubka F, Schießl S P, Gannott F and Zaumseil J 2014 Mapping charge-carrier density across the p–n junction in ambipolar carbon-nanotube networks by Raman microscopy *Adv. Mater.* **26** 7986–92
[90] Jakubka F, Grimm S B, Zakharko Y, Gannott F and Zaumseil J 2014 Trion electroluminescence from semiconducting carbon nanotubes *ACS Nano* **8** 8477–86
[91] Engel M, Small J P, Steiner M, Freitag M, Green A A, Hersam M C and Avouris P 2008 Thin film nanotube transistors based on self-assembled, aligned, semiconducting carbon nanotube arrays *ACS Nano* **2** 2445–52
[92] Shastry T A, Seo J-W T, Lopez J J, Arnold H N, Kelter J Z, Sangwan V K, Lauhon L J, Marks T J and Hersam M C 2013 Large-area, electronically monodisperse, aligned single-walled carbon nanotube thin films fabricated by evaporation-driven self-assembly *Small* **9** 45–51
[93] Li H, Hain T C, Muzha A, Schöppler F and Hertel T 2014 Dynamical contact line pinning and zipping during carbon nanotube coffee stain formation *ACS Nano* **8** 6417–24
[94] Joo Y, Brady G J, Arnold M S and Gopalan P 2014 Dose-controlled, floating evaporative self-assembly and alignment of semiconducting carbon nanotubes from organic solvents *Langmuir* **30** 3460–6
[95] Cao Q, Han S-J, Tulevski G S, Zhu Y, Lu D D and Haensch W 2013 Arrays of single-walled carbon nanotubes

with full surface coverage for high-performance electronics *Nature Nanotech.* **8** 180–6
[96] Baeg K-J, Caironi M and Noh Y-Y 2013 Toward printed integrated circuits based on unipolar or ambipolar polymer semiconductors *Adv. Mater.* **25** 4210–44
[97] Kordás K, Mustonen T, Tóth G, Jantunen H, Lajunen M, Soldano C, Talapatra S, Kar S, Vajtai R and Ajayan P M 2006 Inkjet printing of electrically conductive patterns of carbon nanotubes *Small* **2** 1021–5
[98] Okimoto H, Takenobu T, Yanagi K, Miyata Y, Shimotani H, Kataura H and Iwasa Y 2010 Tunable carbon nanotube thin-film transistors produced exclusively via inkjet printing *Adv. Mater.* **22** 3981–6
[99] Denneulin A, Bras J, Carcone F, Neuman C and Blayo A 2011 Impact of ink formulation on carbon nanotube network organization within inkjet printed conductive films *Carbon* **49** 2603–14
[100] Nobusa Y, Yomogida Y, Matsuzaki S, Yanagi K, Kataura H and Takenobu T 2011 Inkjet printing of single-walled carbon nanotube thin-film transistors patterned by surface modification *Appl. Phys. Lett.* **99** 183106–3
[101] Lee C W, Raman Pillai S K, Luan X, Wang Y, Li C M and Chan-Park M B 2012 High-performance inkjet printed carbon nanotube thin film transistors with high-k HfO2 dielectric on plastic substrate *Small* **8** 2941–7
[102] Zhao J, Gao Y, Gu W, Wang C, Lin J, Chen Z and Cui Z 2012 Fabrication and electrical properties of all-printed carbon nanotube thin film transistors on flexible substrates *J. Mater. Chem.* **22** 20747–53
[103] Kim B, Jang S, Prabhumirashi P L, Geier M L, Hersam M C and Dodabalapur A 2013 Low voltage, high performance inkjet printed carbon nanotube transistors with solution processed ZrO2 gate insulator *Appl. Phys. Lett.* **103** 082119
[104] Vaillancourt J *et al* 2008 All ink-jet-printed carbon nanotube thin-film transistor on a polyimide substrate with an ultrahigh operating frequency of over 5 GHz *Appl. Phys. Lett.* **93** 243301
[105] Ha M, Xia Y, Green A A, Zhang W, Renn M J, Kim C H, Hersam M C and Frisbie C D 2010 Printed, sub-3 V digital circuits on plastic from aqueous carbon nanotube inks *ACS Nano* **4** 4388–95
[106] Ha M, Seo J-W T, Prabhumirashi P L, Zhang W, Geier M L, Renn M J, Kim C H, Hersam M C and Frisbie C D 2013 Aerosol Jet printed, low voltage, electrolyte gated carbon nanotube ring oscillators with sub-5 μs stage delays *Nano Lett.* **13** 954–60
[107] Qian L, Xu W, Fan X, Wang C, Zhang J, Zhao J and Cui Z 2013 Electrical and photoresponse properties of printed thin-film transistors based on poly(9, 9-dioctylfluorene-co-bithiophene) sorted large-diameter semiconducting carbon nanotubes *J. Phys. Chem.* C **117** 18243–50
[108] Liu Z, Zhao J, Xu W, Qian L, Nie S and Cui Z 2014 Effect of surface wettability properties on the electrical properties of printed carbon nanotube thin-film transistors on SiO2/Si substrates *ACS Appl. Mater. Interfaces* **6** 9997–10004
[109] Xu W, Liu Z, Zhao J, Xu W, Gu W, Zhang X, Qian L and Cui Z 2014 Flexible logic circuits based on top-gate thin film transistors with printed semiconductor carbon nanotubes and top electrodes *Nanoscale* **6** 14891–7
[110] Takagi Y, Nobusa Y, Gocho S, Kudou H, Yanagi K, Kataura H and Takenobu T 2013 Inkjet printing of aligned single-walled carbon-nanotube thin films *Appl. Phys. Lett.* **102** 143107
[111] Barman S N, LeMieux M C, Baek J, Rivera R and Bao Z N 2010 Effects of dispersion conditions of single-walled carbon nanotubes on the electrical characteristics of thin film network transistors *ACS Appl. Mater. Interfaces* **2** 2672–8
[112] Nirmalraj P N, Lyons P E, De S, Coleman J N and Boland J J 2009 Electrical connectivity in single-walled carbon nanotube networks *Nano Lett.* **9** 3890–5
[113] Han J-H and Strano M S 2014 Room temperature carrier transport through large diameter bundles of semiconducting single-walled carbon nanotube *Mater. Res. Bull.* **58** 1–5
[114] Znidarsic A, Kaskela A, Laiho P, Gaberscek M, Ohno Y, Nasibulin A G, Kauppinen E I and Hassanien A 2013 Spatially resolved transport properties of pristine and doped single-walled carbon nanotube networks *J. Phys. Chem.* C **117** 13324–30
[115] Søndergaard R R, Hösel M and Krebs F C 2013 Roll-to-roll fabrication of large area functional organic materials *J. Polym. Sci.* **51** 16–34
[116] Du J, Pei S, Ma L and Cheng H-M 2014 25th anniversary article: carbon nanotube- and graphene-based transparent conductive films for optoelectronic devices *Adv. Mater.* **26** 1958–91
[117] Wu Z C *et al* 2004 Transparent, conductive carbon nanotube films *Science* **305** 1273–6
[118] Hecht D S, Hu L and Irvin G 2011 Emerging transparent electrodes based on thin films of carbon nanotubes, graphene, and metallic nanostructures *Adv. Mater.* **23** 1482–513
[119] van de Lagemaat J, Barnes T M, Rumbles G, Shaheen S E, Coutts T J, Weeks C, Levitsky I, Peltola J and Glatkowski P 2006 Organic solar cells with carbon nanotubes replacing In2O3:Sn as the transparent electrode *Appl. Phys. Lett.* **88** 233503
[120] Pasquier A D, Unalan H E, Kanwal A, Miller S and Chhowalla M 2005 Conducting and transparent single-wall carbon nanotube electrodes for polymer-fullerene solar cells *Appl. Phys. Lett.* **87** 203511
[121] Rowell M W, Topinka M A, McGehee M D, Prall H-J, Dennler G, Sariciftci N S, Hu L and Gruner G 2006 Organic solar cells with carbon nanotube network electrodes *Appl. Phys. Lett.* **88** 233506
[122] Cho D-Y, Eun K, Choa S-H and Kim H-K 2014 Highly flexible and stretchable carbon nanotube network electrodes prepared by simple brush painting for cost-effective flexible organic solar cells *Carbon* **66** 530–8
[123] Hu L, Li J, Liu J, Grüner G and Marks T 2010 Flexible organic light-emitting diodes with transparent carbon nanotube electrodes: problems and solutions *Nanotechnology* **21** 155202
[124] Chien Y-M, Lefevre F, Shih I and Izquierdo R 2010 A solution processed top emission OLED with transparent carbon nanotube electrodes *Nanotechnology* **21** 134020
[125] Falco A, Cinà L, Scarpa G, Lugli P and Abdellah A 2014 Fully-sprayed and flexible organic photodiodes with transparent carbon nanotube electrodes *ACS Applied Materials & Interfaces* **6** 10593–601
[126] Azoz S, Exarhos A L, Marquez A, Gilbertson L M, Nejati S, Cha J J, Zimmerman J B, Kikkawa J M and Pfefferle L D 2014 Highly conductive single-walled carbon nanotube thin film preparation by direct alignment on substrates from water dispersions *Langmuir* **31** 1155–63
[127] Blackburn J L, Barnes T M, Beard M C, Kim Y-H, Tenent R C, McDonald T J, To B, Coutts T J and Heben M J 2008 Transparent conductive single-walled carbon nanotube networks with precisely tunable ratios of semiconducting and metallic nanotubes *ACS Nano* **2** 1266–74
[128] Yoon H, Yamashita M, Ata S, Futaba D N, Yamada T and Hata K 2014 Controlling exfoliation in order to minimize damage during dispersion of long SWCNTs for advanced composites *Sci. Rep.* **4** 3907
[129] Fogden S, Howard C A, Heenan R K, Skipper N T and Shaffer M S P 2011 Scalable method for the reductive

dissolution, purification, and separation of single-walled carbon nanotubes *ACS Nano* **6** 54–62
[130] Ostfeld A E, Catheline A, Ligsay K, Kim K-C, Chen Z, Facchetti A, Fogden S and Arias A C 2014 Single-walled carbon nanotube transparent conductive films fabricated by reductive dissolution and spray coating for organic photovoltaics *Appl. Phys. Lett.* **105** 253301
[131] Gwinner M C, Jakubka F, Gannott F, Sirringhaus H and Zaumseil J 2012 Enhanced ambipolar charge injection with semiconducting polymer/carbon nanotube thin films for light-emitting transistors *ACS Nano* **6** 539–48
[132] Yun D-J, Hong K, Kim S h, Yun W-M, Jang J-Y, Kwon W-S, Park C-E and Rhee S-W 2011 Multiwall carbon nanotube and poly(3, 4-ethylenedioxythiophene): polystyrene sulfonate (PEDOT:PSS) composite films for transistor and inverter devices *ACS Appl. Mater. Interfaces* **3** 43–9
[133] Lefenfeld M, Blanchet G and Rogers J A 2003 High-performance contacts in plastic transistors and logic gates that use printed electrodes of DNNSA-PANI doped with single-walled carbon nanotubes *Adv. Mater.* **15** 1188–91
[134] Hellstrom S L, Jin R Z, Stoltenberg R M and Bao Z 2010 Driving high-performance n- and p-type organic transistors with carbon nanotube/conjugated polymer composite electrodes patterned directly from solution *Adv. Mater.* **22** 4204–8
[135] Sun D-M, Timmermans M Y, Kaskela A, Nasibulin A G, Kishimoto S, Mizutani T, Kauppinen E I and Ohno Y 2013 Mouldable all-carbon integrated circuits *Nat. Commun.* **4** 2302
[136] Cao Q, Hur S H, Zhu Z T, Sun Y G, Wang C J, Meitl M A, Shim M and Rogers J A 2006 Highly bendable, transparent thin-film transistors that use carbon-nanotube-based conductors and semiconductors with elastomeric dielectrics *Adv. Mater.* **18** 304–9
[137] Natali D and Caironi M 2012 Charge injection in solution-processed organic field-effect transistors: physics, models and characterization methods *Adv. Mater.* **24** 1357–87
[138] Cicoira F, Aguirre C M and Martel R 2011 Making contacts to n-type organic transistors using carbon nanotube arrays *ACS Nano* **5** 283–90
[139] Cicoira F, Coppede N, Iannotta S and Martel R 2011 Ambipolar copper phthalocyanine transistors with carbon nanotube array electrodes *Appl. Phys. Lett.* **98** Art. No.183303
[140] Aguirre C M, Ternon C, Paillet M, Desjardins P and Martel R 2009 Carbon nanotubes as injection electrodes for organic thin film transistors *Nano Lett.* **9** 1457–61
[141] Kang N, Sarker B K and Khondaker S I 2012 The effect of carbon nanotube/organic semiconductor interfacial area on the performance of organic transistors *Appl. Phys. Lett.* **101** 233302–4
[142] Sarker B K and Khondaker S I 2012 Thermionic emission and tunneling at carbon nanotube–organic semiconductor interface *ACS Nano* **6** 4993–9
[143] Xie W *et al* 2013 Utilizing carbon nanotube electrodes to improve charge injection and transport in bis (trifluoromethyl)-dimethyl-rubrene (fm-rubrene) ambipolar single crystal transistors *ACS Nano* **7** 10245–56
[144] Wang M, Jakubka F, Gannott F, Schweiger M and Zaumseil J 2014 Generalized enhancement of charge injection in bottom contact/top gate polymer field-effect transistors with single-walled carbon nanotubes *Org. Electron.* **15** 809–17
[145] Zaumseil J, Donley C L, Kim J S, Friend R H and Sirringhaus H 2006 Efficient top-gate, ambipolar, light-emitting field-effect transistors based on a green-light-emitting polyfluorene *Adv. Mater.* **18** 2708–12
[146] Liu B, McCarthy M A, Yoon Y, Kim D Y, Wu Z C, So F, Holloway P H, Reynolds J R, Guo J and Rinzler A G 2008 Carbon-nanotube-enabled vertical field effect and light-emitting transistors *Adv. Mater.* **20** 3605–9
[147] McCarthy M A, Liu B and Rinzler A G 2010 High current, low voltage carbon nanotube enabled vertical organic field effect transistors *Nano Lett.* **10** 3467–72
[148] McCarthy M A, Liu B, Donoghue E P, Kravchenko I, Kim D Y, So F and Rinzler A G 2011 Low-voltage, low-power, organic light-emitting transistors for active matrix displays *Science* **332** 570–3
[149] Ben-Sasson A J, Avnon E, Ploshnik E, Globerman O, Shenhar R, Frey G L and Tessler N 2009 Patterned electrode vertical field effect transistor fabricated using block copolymer nanotemplates *Appl. Phys. Lett.* **95** 213301
[150] Ben-Sasson A J and Tessler N 2012 Unraveling the physics of vertical organic field effect transistors through nanoscale engineering of a self-assembled transparent electrode *Nano Lett.* **12** 4729–33
[151] Ye Y, Bindl D J, Jacobberger R M, Wu M-Y, Roy S S and Arnold M S 2014 Semiconducting carbon nanotube aerogel bulk heterojunction solar cells *Small* **10** 3299–306
[152] Tune D D and Shapter J G 2013 The potential sunlight harvesting efficiency of carbon nanotube solar cells *Energy Environ. Sci.* **6** 2572–7
[153] Dowgiallo A-M, Mistry K S, Johnson J C and Blackburn J L 2014 Ultrafast spectroscopic signature of charge transfer between single-walled carbon nanotubes and C60 *ACS Nano* **8** 8573–81
[154] Shea M J and Arnold M S 2013 1% solar cells derived from ultrathin carbon nanotube photoabsorbing films *Appl. Phys. Lett.* **102** 243101
[155] Bindl D J, Wu M-Y, Prehn F C and Arnold M S 2010 Efficiently harvesting excitons from electronic type-controlled semiconducting carbon nanotube films *Nano Lett.* **11** 455–60
[156] Jain R M, Howden R, Tvrdy K, Shimizu S, Hilmer A J, McNicholas T P, Gleason K K and Strano M S 2012 Polymer-free near-infrared photovoltaics with single chirality (6, 5) semiconducting carbon nanotube active layers *Adv. Mater.* **24** 4436–9
[157] Gong M, Shastry T A, Xie Y, Bernardi M, Jasion D, Luck K A, Marks T J, Grossman J C, Ren S and Hersam M C 2014 Polychiral semiconducting carbon nanotube–fullerene solar cells *Nano Lett.* **14** 5308–14
[158] Reyes-Reyes M, Kim K and Carroll D L 2005 High-efficiency photovoltaic devices based on annealed poly(3-hexylthiophene) and 1-(3-methoxycarbonyl)-propyl-1-phenyl-(6, 6)C61 blends *Appl. Phys. Lett.* **87** 083506
[159] Chen Z H, Appenzeller J, Lin Y M, Sippel-Oakley J, Rinzler A G, Tang J Y, Wind S J, Solomon P M and Avouris P 2006 An integrated logic circuit assembled on a single carbon nanotube *Science* **311** 1735
[160] Franklin A D, Luisier M, Han S-J, Tulevski G, Breslin C M, Gignac L, Lundstrom M S and Haensch W 2012 Sub-10 nm carbon nanotube transistor *Nano Lett.* **12** 758–62
[161] Appenzeller J, Knoch J, Martel R, Derycke V, Wind S J and Avouris P 2002 Carbon nanotube electronics *IEEE Trans. Nanotechnol.* **1** 184–9
[162] Kumar S, Murthy J Y and Alam M A 2005 Percolating conduction in finite nanotube networks *Phys. Rev. Lett.* **95** 066802
[163] Kocabas C, Pimparkar N, Yesilyurt O, Kang S J, Alam M A and Rogers J A 2007 Experimental and theoretical studies of transport through large scale, partially aligned arrays of single-walled carbon nanotubes in thin film type transistors *Nano Lett.* **7** 1195–202
[164] Pimparkar N, Cao Q, Rogers J A and Alam M A 2009 Theory and practice of 'striping' for improved on/off ratio in carbon nanonet thin film transistors *Nano Research* **2** 167–75

[165] Rouhi N, Jain D and Burke P J 2011 High-performance semiconducting nanotube inks: progress and prospects *ACS Nano* **5** 8471–87
[166] Sirringhaus H 2014 25th Anniversary article: organic field-effect transistors: the path beyond amorphous silicon *Adv. Mater.* **26** 1319–35
[167] Gelinck G, Heremans P, Nomoto K and Anthopoulos T D 2010 Organic transistors in optical displays and microelectronic applications *Adv. Mater.* **22** 3778–98
[168] Asada Y, Miyata Y, Shiozawa K, Ohno Y, Kitaura R, Mizutani T and Shinohara H 2010 Thin-Film transistors with length-sorted DNA-wrapped single-wall carbon nanotubes *J. Phys. Chem.* C **115** 270–3
[169] Snow E S, Novak J P, Campbell P M and Park D 2003 Random networks of carbon nanotubes as an electronic material *Appl. Phys. Lett.* **82** 2145–7
[170] Snow E S, Campbell P M, Ancona M G and Novak J P 2005 High-mobility carbon-nanotube thin-film transistors on a polymeric substrate *Appl. Phys. Lett.* **86** 033105
[171] Asada Y, Miyata Y, Ohno Y, Kitaura R, Sugai T, Mizutani T and Shinohara H 2010 High-performance thin-film transistors with dna-assisted solution processing of isolated single-walled carbon nanotubes *Adv. Mater.* **22** 2698–701
[172] Cao Q, Han S-J, Tulevski G S, Franklin A D and Haensch W 2012 Evaluation of field-effect mobility and contact resistance of transistors that use solution-processed single-walled carbon nanotubes *ACS Nano* **6** 6471–7
[173] Bisri S Z, Gao J, Derenskyi V, Gomulya W, Iezhokin I, Gordiichuk P, Herrmann A and Loi M A 2012 High performance ambipolar field-effect transistor of random network carbon nanotubes *Adv. Mater.* **24** 6147–52
[174] Wang H *et al* 2014 Tuning the threshold voltage of carbon nanotube transistors by n-type molecular doping for robust and flexible complementary circuits *Proc. Natl. Acad. Sci. USA* **111** 4776–81
[175] Ding J *et al* 2014 Enrichment of large-diameter semiconducting SWCNTs by polyfluorene extraction for high network density thin film transistors *Nanoscale* **6** 2328–39
[176] Brady G J, Joo Y, Wu M-Y, Shea M J, Gopalan P and Arnold M S 2014 Polyfluorene-sorted, carbon nanotube array field-effect transistors with increased current density and high on/off ratio *ACS Nano* **8** 11614–21
[177] Sangwan V K, Ortiz R P, Alaboson J M P, Emery J D, Bedzyk M J, Lauhon L J, Marks T J and Hersam M C 2012 Fundamental performance limits of carbon nanotube thin-film transistors achieved using hybrid molecular dielectrics *ACS Nano* **6** 7480–8
[178] Zhao Y, Candebat D, Delker C, Zi Y, Janes D, Appenzeller J and Yang C 2012 Understanding the impact of schottky barriers on the performance of narrow bandgap nanowire field effect transistors *Nano Lett.* **12** 5331–6
[179] Franklin A D, Farmer D B and Haensch W 2014 Defining and overcoming the contact resistance challenge in scaled carbon nanotube transistors *ACS Nano* **8** 7333–9
[180] Fuhrer M S, Lim A K L, Shih L, Varadarajan U, Zettl A and McEuen P L 2000 Transport through crossed nanotubes *Physica* E **6** 868–71
[181] Sze S M 2002 *Semiconductor Devices—Physics and Technology* (New York: John Wiley & Sons)
[182] Rosenblatt S, Yaish Y, Park J, Gore J, Sazonova V and McEuen P L 2002 High performance electrolyte gated carbon nanotube transistors *Nano Lett.* **2** 869–72
[183] Cao Q, Xia M G, Kocabas C, Shim M, Rogers J A and Rotkin S V 2007 Gate capacitance coupling of singled-walled carbon nanotube thin-film transistors *Appl. Phys. Lett.* **90** 023516
[184] Halik M, Klauk H, Zschieschang U, Schmid G, Dehm C, Schutz M, Maisch S, Effenberger F, Brunnbauer M and Stellacci F 2004 Low-voltage organic transistors with an amorphous molecular gate dielectric *Nature* **431** 963–6
[185] Weitz R T, Zschieschang U, Effenberger F, Klauk H, Burghard M and Kern K 2007 High-performance carbon nanotube field effect transistors with a thin gate dielectric based on a self-assembled monolayer *Nano Lett.* **7** 22–7
[186] Kim W, Javey A, Vermesh O, Wang O, Li Y M and Dai H J 2003 Hysteresis caused by water molecules in carbon nanotube field-effect transistors *Nano Lett.* **3** 193–8
[187] Aguirre C M, Levesque P L, Paillet M, Lapointe F, St-Antoine B C, Desjardins P and Martel R 2009 The role of the oxygen/water redox couple in suppressing electron conduction in field-effect transistors *Adv. Mater.* **21** 3087–91
[188] Qian Q, Li G, Jin Y, Liu J, Zou Y, Jiang K, Fan S and Li Q 2014 Trap-state-dominated suppression of electron conduction in carbon nanotube thin-film transistors *ACS Nano* **8** 9597–605
[189] Wang H, Cobb B, van Breemen A, Gelinck G and Bao Z 2014 Highly stable carbon nanotube top-gate transistors with tunable threshold voltage *Adv. Mater.* **26** 4588–93
[190] Ha T-J, Kiriya D, Chen K and Javey A 2014 Highly stable hysteresis-free carbon nanotube thin-film transistors by fluorocarbon polymer encapsulation *ACS Appl. Mater. Interfaces* **6** 8441–6
[191] Jang S, Kim B, Geier M L, Prabhumirashi P L, Hersam M C and Dodabalapur A 2014 Fluoropolymer coatings for improved carbon nanotube transistor device and circuit performance *Appl. Phys. Lett.* **105** 122107
[192] Martel R, Schmidt T, Shea H R, Hertel T and Avouris P 1998 Single- and multi-wall carbon nanotube field-effect transistors *Appl. Phys. Lett.* **73** 2447–9
[193] Shim M, Javey A, Kam N W S and Dai H J 2001 Polymer functionalization for air-stable n-type carbon nanotube field-effect transistors *J. Am. Chem. Soc.* **123** 11512–3
[194] Lee S Y, Lee S W, Kim S M, Yu W J, Jo Y W and Lee Y H 2011 Scalable complementary logic gates with chemically doped semiconducting carbon nanotube transistors *ACS Nano* **5** 2369–75
[195] Kang B R *et al* 2009 Restorable type conversion of carbon nanotube transistor using pyrolytically controlled antioxidizing photosynthesis coenzyme *Adv. Funct. Mater.* **19** 2553–9
[196] Derycke V, Martel R, Appenzeller J and Avouris P 2001 Carbon nanotube inter- and intramolecular logic gates *Nano Lett.* **1** 453–6
[197] Ha T-J, Chen K, Chuang S, Yu K M, Kiriya D and Javey A 2014 Highly uniform and stable n-type carbon nanotube transistors by using positively charged silicon nitride thin films *Nano Lett.* **15** 392–7
[198] Venkateshvaran D *et al* 2014 Approaching disorder-free transport in high-mobility conjugated polymers *Nature* **515** 384–8
[199] Chen P, Fu Y, Aminirad R, Wang C, Zhang J, Wang K, Galatsis K and Zhou C 2011 Fully printed separated carbon nanotube thin film transistor circuits and its application in organic light emitting diode control *Nano Lett.* **11** 5301–8
[200] Zhang J, Wang C and Zhou C 2012 Rigid/flexible transparent electronics based on separated carbon nanotube thin-film transistors and their application in display electronics *ACS Nano* **6** 7412–9
[201] Zhang J, Fu Y, Wang C, Chen P-C, Liu Z, Wei W, Wu C, Thompson M E and Zhou C 2011 Separated carbon nanotube macroelectronics for active matrix organic light-emitting diode displays *Nano Lett.* **11** 4852–8
[202] Takahashi T, Yu Z, Chen K, Kiriya D, Wang C, Takei K, Shiraki H, Chen T, Ma B and Javey A 2013 Carbon nanotube active-matrix backplanes for mechanically flexible visible light and x-ray imagers *Nano Lett.* **13** 5425–30

[203] Yeom C, Chen K, Kiriya D, Yu Z, Cho G and Javey A 2015 Large-area compliant tactile sensors using printed carbon nanotube active-matrix backplanes *Adv. Mater.* **27** 1561–6
[204] Xu F, Wu M-Y, Safron N S, Roy S S, Jacobberger R M, Bindl D J, Seo J-H, Chang T-H, Ma Z and Arnold M S 2014 Highly stretchable carbon nanotube transistors with ion gel gate dielectrics *Nano Lett.* **14** 682–6
[205] Lee K H, Kang M S, Zhang S, Gu Y, Lodge T P and Frisbie C D 2012 'Cut and stick' rubbery ion gels as high capacitance gate dielectrics *Adv. Mater.* **24** 4457–62
[206] Kim S H, Hong K, Xie W, Lee K H, Zhang S, Lodge T P and Frisbie C D 2012 Electrolyte-gated transistors for organic and printed electronics *Adv. Mater.* **25** 1822–46
[207] Ozel T, Gaur A, Rogers J A and Shim M 2005 Polymer electrolyte gating of carbon nanotube network transistors *Nano Lett.* **5** 905–11
[208] Shimotani H, Tsuda S, Yuan H, Yomogida Y, Moriya R, Takenobu T, Yanagi K and Iwasa Y 2014 Continuous band-filling control and one-dimensional transport in metallic and semiconducting carbon nanotube tangled films *Adv. Funct. Mater.* **24** 3305–11
[209] Siddons G P, Merchin D, Back J H, Jeong J K and Shim M 2004 Highly efficient gating and doping of carbon nanotubes with polymer electrolytes *Nano Lett.* **4** 927–31
[210] Cho J H, Lee J, Xia Y, Kim B, He Y Y, Renn M J, Lodge T P and Frisbie C D 2008 Printable ion-gel gate dielectrics for low-voltage polymer thin-film transistors on plastic *Nat. Mater.* **7** 900–6
[211] Hong K, Kim Y H, Kim S H, Xie W, Xu W D, Kim C H and Frisbie C D 2014 Aerosol jet printed, sub-2 V complementary circuits constructed from P- and N-type electrolyte gated transistors *Adv. Mater.* **26** 7032–7
[212] Thiemann S, Sachnov S J, Pettersson F, Bollström R, Österbacka R, Wasserscheid P and Zaumseil J 2014 Cellulose-based ionogels for paper electronics *Adv. Funct. Mater.* **24** 625–34
[213] Pu J, Yomogida Y, Liu K-K, Li L-J, Iwasa Y and Takenobu T 2012 Highly flexible MoS2 thin-film transistors with ion gel dielectrics *Nano Lett.* **12** 4013–7
[214] Geier M L, Prabhumirashi P L, McMorrow J J, Xu W, Seo J-W T, Everaerts K, Kim C H, Marks T J and Hersam M C 2013 Subnanowatt carbon nanotube complementary logic enabled by threshold voltage control *Nano Lett.* **13** 4810–4
[215] Zhang J, Wang C, Fu Y, Che Y and Zhou C 2011 Air-stable conversion of separated carbon nanotube thin-film transistors from p-type to n-type using atomic layer deposition of high-k oxide and its application in CMOS logic circuits *ACS Nano* **5** 3284–92
[216] Jinsoo N, Minhun J, Kyunghwan J, Soyeon L, Gwangyong L, Subramanian V, Leonard A D, Tour J and Gyoujin C 2010 Modeling of printed single walled carbon nanotube thin film transistors for attaining optimized clock signals *J. Appl. Phys.* **108** 102811–7
[217] Noh J, Jung M, Jung K, Lee G, Lim S, Kim D, Kim S, Tour J M and Cho G 2011 Integrable single walled carbon nanotube (SWNT) network based thin film transistors using roll-to-roll gravure and inkjet *Organic Electronics* **12** 2185–91
[218] Wang C, Zhang J and Zhou C 2010 Macroelectronic integrated circuits using high-performance separated carbon nanotube thin-film transistors *ACS Nano* **4** 7123–32
[219] Sun D-M, Timmermans M Y, Tian Y, Nasibulin A G, Kauppinen E I, Kishimoto S, Mizutani T and Ohno Y 2011 Flexible high-performance carbon nanotube integrated circuits *Nat. Nanotechnol.* **6** 156–61
[220] Jinsoo N *et al* 2011 Fully gravure-printed D flip-flop on plastic foils using single-walled carbon-nanotube-based TFTs *Electron Device Lett., IEEE* **32** 638–40
[221] Jung M *et al* 2010 All-printed and roll-to-roll-printable 13.56 MHz-operated 1-bit RF tag on plastic foils *IEEE Trans. Electron Devices* **57** 571–80
[222] Kim B, Jang S, Geier M L, Prabhumirashi P L, Hersam M C and Dodabalapur A 2014 High-speed, inkjet-printed carbon nanotube/zinc tin oxide hybrid complementary ring oscillators *Nano Lett.* **14** 3683–7
[223] Shulaker M M, Hills G, Patil N, Wei H, Chen H-Y, Wong H S P and Mitra S 2013 Carbon nanotube computer *Nature* **501** 526–30
[224] Chen J, Perebeinos V, Freitag M, Tsang J, Fu Q, Liu J and Avouris P 2005 Bright infrared emission from electrically induced excitons in carbon nanotubes *Science* **310** 1171–4
[225] Freitag M, Perebeinos V, Chen J, Stein A, Tsang J C, Misewich J A, Martel R and Avouris P 2004 Hot carrier electroluminescence from a single carbon nanotube *Nano Lett.* **4** 1063–6
[226] Adam E, Aguirre C M, Marty L, St-Antoine B C, Meunier F, Desjardins P, Menard D and Martel R 2008 Electroluminescence from single-wall carbon nanotube network transistors *Nano Lett.* **8** 2351–5
[227] Freitag M, Chen J, Tersoff J, Tsang J C, Fu Q, Liu J and Avouris P 2004 Mobile ambipolar domain in carbon-nanotube infrared emitters *Phys. Rev. Lett.* **93** 076803
[228] Jakubka F, Backes C, Gannott F, Mundloch U, Hauke F, Hirsch A and Zaumseil J 2013 Mapping charge transport by electroluminescence in chirality-selected carbon nanotube networks *ACS Nano* **7** 7428–35
[229] Tsyboulski D A, Rocha J D R, Bachilo S M, Cognet L and Weisman R B 2007 Structure-dependent fluorescence efficiencies of individual single-walled cardon nanotubes *Nano Lett.* **7** 3080–5
[230] Cherukuri T K, Tsyboulski D A and Weisman R B 2012 Length- and defect-dependent fluorescence efficiencies of individual single-walled carbon nanotubes *ACS Nano* **6** 843–50
[231] Hertel T, Himmelein S, Ackermann T, Stich D and Crochet J 2011 Diffusion Limited photoluminescence quantum yields in 1-D semiconductors: single-wall carbon nanotubes *ACS Nano* **4** 7161–8
[232] Lefebvre J, Fraser J M, Finnie P and Homma Y 2004 Photoluminescence from an individual single-walled carbon nanotube *Phys. Rev.* B **69** 075403
[233] Kiowski O, Lebedkin S, Hennrich F, Malik S, Rosner H, Arnold K, Surgers C and Kappes M M 2007 Photoluminescence microscopy of carbon nanotubes grown by chemical vapor deposition: Influence of external dielectric screening on optical transition energies *Phys. Rev.* B **75** 7
[234] Welsher K, Sherlock S P and Dai H 2011 Deep-tissue anatomical imaging of mice using carbon nanotube fluorophores in the second near-infrared window *Proc. Natl. Acad. Sci. USA* **108** 8943–8
[235] Hong G *et al* 2014 Through-skull fluorescence imaging of the brain in a new near-infrared window *Nat. Photonics* **8** 723–30
[236] Avouris P, Freitag M and Perebeinos V 2008 Carbon-nanotube photonics and optoelectronics *Nat. Photon.* **2** 341–50
[237] Gaufrès E, Izard N, Noury A, Le Roux X, Rasigade G, Beck A and Vivien L 2012 Light emission in silicon from carbon nanotubes *ACS Nano* **6** 3813–9
[238] Khasminskaya S, Pyatkov F, Flavel B S, Pernice W H and Krupke R 2014 Waveguide-integrated light-emitting carbon nanotubes *Adv. Mater.* **26** 3465–72
[239] Mueller T, Kinoshita M, Steiner M, Perebeinos V, Bol A A, Farmer D B and Avouris P 2009 Efficient narrow-band light emission from a single carbon nanotube p-n diode *Nat. Nanotechnol.* **5** 27–31

[240] Kinoshita M, Steiner M, Engel M, Small J P, Green A A, Hersam M C, Krupke R, Mendez E E and Avouris P 2010 The polarized carbon nanotube thin film LED *Opt. Express* **18** 25738–45

[241] Schornbaum J, Zakharko Y, Held M, Thiemann S, Gannott F and Zaumseil J 2015 Light-emitting quantum dot transistors: emission at high charge carrier densities *Nano Lett.* **15** 1822–8

[242] Tersoff J, Freitag M, Tsang J C and Avouris P 2005 Device modeling of long-channel nanotube electro-optical emitter *Appl. Phys. Lett.* **86** 263108

[243] Matsunaga R, Matsuda K and Kanemitsu Y 2011 Observation of charged excitons in hole-doped carbon nanotubes using photoluminescence and absorption spectroscopy *Phys. Rev. Lett.* **106** 037404

[244] Park J S, Hirana Y, Mouri S, Miyauchi Y, Nakashima N and Matsuda K 2012 Observation of negative and positive trions in the electrochemically carrier-doped single-walled carbon nanotubes *J. Am. Chem. Soc.* **134** 14461–6

[245] Freitag M, Tsang J C, Kirtley J, Carlsen A, Chen J, Troeman A, Hilgenkamp H and Avouris P 2006 Electrically excited, localized infrared emission from single carbon nanotubes *Nano Lett.* **6** 1425–33

[246] Xia F N, Steiner M, Lin Y M and Avouris P 2008 A microcavity-controlled, current-driven, on-chip nanotube emitter at infrared wavelengths *Nat. Nanotechnol.* **3** 609–13

[247] Yu D, Liu H, Peng L-M and Wang S 2015 Flexible light-emitting devices based on chirality-sorted semiconducting carbon nanotube films *ACS Appl. Mater. Interfaces* **7** 3462–7

[248] Hibino N, Suzuki S, Wakahara H, Kobayashi Y, Sato T and Maki H 2011 Short-wavelength electroluminescence from single-walled carbon nanotubes with high bias voltage *ACS Nano* **5** 1215–22

[249] Lefebvre J, Austing D G and Finnie P 2009 Two modes of electroluminescence from single-walled carbon nanotubes *Phys. Status Solidi RRL* **3** 199–201

[250] Pfeiffer M H P, Stürzl N, Marquardt C W, Engel M, Dehm S, Hennrich F, Kappes M M, Lemmer U and Krupke R 2011 Electroluminescence from chirality-sorted (9, 7)-semiconducting carbon nanotube devices *Opt. Express* **19** A1184–9